MEERTENS MODULATION OF PPARα ACTIVITY BY mtHMG-CoAS M.Sc.

MODULATION OF PEROXISOME PROLIFERATOR-ACTIVATED RECEPTOR α ACTIVITY BY MITOCHONDRIAL 3-HYDROXY-3-METHYLGLUTARYL COENZYME A SYNTHASE

By

LISA MEERTENS, B.Sc.

A Thesis

Submitted to the School of Graduate Studies

in Partial Fulfilment of the Requirements

for the Degree

Master of Science

McMaster University

MASTER OF SCIENCE (1998) (Biochemistry)	McMaster University Hamilton, Ontario
TITLE:	Modulation of Peroxisome Proliferator-Activated Receptor α Activity by Mitochondrial 3-Hydroxy-3-Methylglutaryl Coenzyme A Synthase
AUTHOR:	Lisa Meertens, B.Sc. (University of Guelph)
SUPERVISOR:	Professor John P. Capone
NUMBER OF PAGES:	xv, 85

ABSTRACT

The regulation of gene expression at the level of transcription is an important mechanism for maintaining homeostasis. The peroxisome proliferator-activated receptor α (PPARα) is a member of the nuclear hormone receptor superfamily that is involved in transcriptionally modulating such pathways as lipid and fatty acid metabolism. This receptor binds to enhancer elements, peroxisome proliferator-responsive elements (PPREs), upstream of a variety of target genes including those involved in β-oxidation of fatty acids, in the peroxisome and mitochondria, and ketogenesis. One such element has been identified upstream of the rat mitochondrial 3-hydroxy-3-methylglutaryl coenzyme A synthase (mtHMG-CoAS) gene. This enzyme has been shown to be one of the key regulatory points of ketogenesis.

To learn how PPARα mediated transcriptional regulation occurs, this receptor was used as bait in a yeast dihybrid screen and was found to interact with human mtHMG-CoAS. Reproduction of this interaction *in vitro* was performed by solid phase capture assays, using GST fusion proteins, and by co-immunoprecipitations. It was also ascertained that the synthase enzyme interacts with the retinoid X receptor α (RXRα). The hamster cytoplasmic form of the enzyme was chosen as a control and showed no binding capabilities to either nuclear hormone receptor.

Interestingly, the mitochondrial enzyme contains a motif, LXXLL that has previously been shown to be important for binding between a transcriptional coactivator

and a receptor. A site-directed mutant of the mitochondrial synthase sequence from LASLL to LASVL was made. The mutant showed a reduced ability to interact with both nuclear receptors. Consequently, the LXXLL motif is responsible, at least in part, for the interaction between mtHMG-CoAS and both PPARα and RXRα. The cytoplasmic synthase does not contain the motif; its corresponding sequence is LASVL.

The effect of the mitochondrial synthase within a cell was then determined by transient transfection assays. It was discovered that on the HMG PPRE the mitochondrial synthase potentiated PPARα mediated transactivation while on the AOx PPRE the enzyme inhibited it. Thus, mtHMG-CoAS modulates PPARα activity in a PPRE dependent manner. The LXXVL mitochondrial mutant inhibited PPARα transactivation on both the HMG and AOx PPRE. Therefore, the mutant acts as a dominant-negative inhibitor of PPARα mediated activity. The cytoplasmic control enzyme had no effect on either PPRE.

To determine if the mitochondrial enzyme could be detected within the nucleus where it appeared to be modulating PPARα mediated transcription, localization studies were performed with the use of immunofluorescence. Immunofluorescence was done by utilizing hemagglutinin (HA) epitope tagged fusions of the mitochondrial, mutant and cytoplasmic enzymes. When the HA tag was placed at the carboxyl terminus of mtHMG-CoAS, the enzyme was localized to the mitochondria with no apparent nuclear staining. This is consistent with previous localization studies done with the rat mtHMG-CoAS. Also, the mutant enzyme, with the HA tag at the carboxyl terminus, was only detected in

the mitochondria. However, under certain conditions, when PPARα and the mitochondrial synthase were co-transfected, the mitochondrial enzyme was detected within both the mitochondria and the nucleus. The mutant, on the other hand, when co-transfected with PPARα was found to remain non-nuclear. The HA tagged cytoplasmic control enzyme was also non-nuclear. Therefore, mtHMG-CoAS can be detected within the nucleus, it binds, due to at least in part a LXXLL motif, to nuclear receptors, and it is capable of modulating transcription in a PPRE dependent manner.

Ketogenesis becomes an important mechanism for fuel production during starvation, prolonged exercise and diabetes. Perhaps, during extreme circumstances such as starvation, mtHMG-CoAS is involved in autoregulation which allows for an amplification of the transcription of its own gene. Also, mtHMG-CoAS appears to inhibit the transcription of the AOx enzyme which is involved in peroxisomal fatty acid β-oxidation. Again, perhaps under extreme conditions, the β-oxidation of fatty acids is concentrated within the mitochondria which allows for the production of acetyl-CoA that can subsequently be converted to ketone bodies that can then be utilized for fuel.

DEDICATIONS

I would like to dedicate this thesis to my parents, John and Judy Meertens and my sister Amy for all of their love and support over the years. Without their encouragement and listening ears, this work could never have been completed. I would like to also dedicate this to my very soon to be husband Jonathan Cechetto. His love, sense of humour and generous gifts of ice cream bars most definitely gave me the strength to carry on.

ACKNOWLEDGEMENTS

I would like to give my sincerest thanks to my supervisor John Capone for all the encouragement, insight and free trips to Lake Tahoe. I will most certainly miss the daily "What's up Lisa?" A special thanks to my committee members David Andrews and John Hassell for their words of advice.

Many thanks to all the lab members both past and present for their riveting lunch time conversation. Pat, Kenji, Jozo, Jamie, Shannon, Mike and John you have all made the time pass quickly. Also, thanks to Shirley and Hansa for all their additional help.

A special thanks to my #1 Loop Buddy (but not best friend) Pat. You being, in essence me, was able to provide a sense of humour and daily support that will genuinely be missed. You cheered me up when I was feeling down, you relaxed me when I was feeling stressed and you were always there for me to vent. Thank-you for being a true friend!

TABLE OF CONTENTS

LIST OF FIGURES

LIST OF TABLES

LIST OF ABBREVIATIONS

aa	amino acid(s)
AOx	acyl-CoA oxidase
APS	ammonium persulphate
ATP	adenosine triphosphate
bp	base pairs
BSA	bovine serum albumin
CBP	CREB-binding protein
cHMG-CoAS	cytoplasmic HMG-CoA synthase
COUP-TF	chicken ovalbumin upstream-promoter transcription factor
CPS	carbamyl-phosphate synthetase
CREB	3′,5′-monophosphate-regulated enhancer binding protein
Cys	cysteine
DBD	DNA binding domain
DNA	deoxyribonucleic acid
dNTPs	deoxyribonucleotide triphosphates
DOC	deoxycholic acid
dsDNA	double stranded DNA
DTT	dithiothreitol
dUTPase	deoxyuridine triphosphatase
EDTA	ethylenediaminetetracetic acid
EMSA	electrophoretic mobility shift assay
GRIP1	glucocorticoid receptor-interacting protein 1
GST	glutathione S-transferase
HA	hemagglutinin
HAc	acetic acid
HEPES	N-(2-Hydroxyethyl)piperazine-N′-(2-ethanesulfonic acid)
HMG-CoA	3-hydroxy-3-methylglutaryl coenzyme A
HNF-4	hepatocyte nuclear factor 4
hr(s)	hour(s)
IPTG	iso-propyl-thiogalactoside
Kb	kilobase pairs
kDa	kilodaltons
LDL	low density lipoprotein
LXR	liver X receptor
MCS	multiple cloning site
mtHMG-CoAS	mitochondrial HMG-CoA synthase
min(s)	minute(s)
MOPS	3-(N-Morpholino)propanesulfonic acid
mPPAR	mouse peroxisome proliferator-activated receptor

N-CoR	nuclear receptor corepressor
NHR	nuclear hormone receptor
NP-40	Nonidet P-40
OD	optical density
PBP	PPAR-binding protein
PBS	phosphate buffered saline
P/CAF	p300/CBP-associated factor
p/CIP	p300/CBP/co-integrator-associated protein
PMSF	phenylmethylsulfonylfluoride
poly-A signal	polyadenylation signal
PPAR	peroxisome proliferator-activated receptor
PPRE	peroxisome proliferator-responsive element
RA	9-*cis* retinoic acid
RAR	retinoid acid receptor
RIP140	receptor-interacting protein 140
RXR	retinoid X receptor
SDS-PAGE	sodium dodecyl sulphate polyacrylamide gel electrophoresis
sec(s)	second(s)
SMRT	silencing mediator (corepressor) for retinoid and thyroid-hormone receptors
ssDNA	single stranded DNA
SRC-1	steroid receptor coactivator-1
TBP	TATA binding protein
TBS	Tris-buffered saline
TBST	Tris-buffered saline Tween 20
TE	Tris-EDTA
TFIIB	transcription factor IIB
TIF2	transcriptional intermediary factor 2
TR	thyroid-hormone receptor
Tris	Tris(Hydroxymethyl)Aminoethane

CHAPTER ONE

INTRODUCTION

1.1 Transcription Overview

Growth, development and homeostasis is controlled within our bodies by a variety of mechanisms, one of which is gene regulation at the level of transcription. Transcription, in eukaryotes, is the copying of one strand of DNA into a complementary RNA sequence by the enzyme RNA Polymerase II. RNA Polymerase II binds to DNA through a specific DNA sequence found within the promoter. RNA Polymerase II binds to DNA with a group of other auxiliary factors such as TBP (TATA binding protein), which binds to a DNA sequence known as the TATA-box and TFIIB (transcription factor IIB) which binds both TBP and RNA Polymerase II. Another group of proteins, known as transactivators, bind to upstream 'enhancer' elements and modulate transcriptional activity. It is believed that transactivators stimulate transcription by aiding in the assembly of the basal transcription factors into a stable pre-initiation complex. By facilitating this assembly, the rate of gene expression is increased. Several of these transactivator receptors interact directly with the components of the basal transcriptional machinery such as TBP and TFIIB (reviewed in Shibata *et al.*, 1997)

1.2 PPARs

1.2.1 Isotypes

Peroxisome proliferator-activated receptors (PPARs) are members of the nuclear hormone receptor superfamily of ligand-activated transcription factors (transactivators) that assist in regulating a wide variety of genes involved in adipocyte differentiation (Tontonoz *et al.*, 1994), lipid and metabolic pathways (reviewed in Schoonjans *et al.*, 1996a,b) and energy utilization (Puigserver *et al.*, 1998). Refer to Table 1 for a list of some of the genes regulated by PPARs.

The first PPAR to be cloned was from the mouse (mPPARα) in 1990 by Isseman and Green. Since then, three different isotypes of PPARs have been cloned; α, β and γ types from Xenopus, α, δ and γ types from the mouse and α and δ types (hNuc1) in humans (reviewed in Green, 1995 and Schoonjans *et al.*, 1996a,b). Two mouse PPARγ isoforms have been identified; PPARγ1 and PPARγ2 that differ in their amino terminal 30 aa due to alternative promoter use and differential splicing (Zhu *et al.*, 1993, Tontonoz *et al.*, 1994, Zhu *et al.*, 1995). In mammals, PPARα is expressed abundantly in liver, heart and kidney whereas PPARδ is more widely expressed (Braissant *et al.*, 1996, reviewed in Schoonjans *et al.*, 1996a,b). PPARγ1 is expressed in similar tissues as PPARα whereas PPARγ2 is found predominantly in adipose tissue and the immune system (Zhu *et al.*, 1993, Braissant *et al.*, 1996, reviewed in Schoonjans *et al.*, 1996a,b).

Table 1: Functional Peroxisome Proliferator-Responsive Elements (PPREs) (modified from Schoonjans *et al.*, 1996b)

Gene	Location	PPRE	Function of Gene
Consensus		TGACCTnTGACCT	
Acyl-CoA oxidase (AOx)	-570/-558 -214/-202	TGACCTtTGTCCT TGACCTtCTACCT	β-oxidation in peroxisome
Bifunctional protein (enoyl-CoA hydratase)	-2939/-2927	TGAACTaTTACCT	β-oxidation in peroxisome
Acyl-CoA synthetase	-175/-154	TGACTGaTGCCCT	Formation of acyl-CoA esters
Cytochome P450IVA6	-650/-662 -728/-740 -27/-1	TCACTTtTGCCCT TGGCCTtTGTCCT TGACCTtTGCCCA	ω-oxidation of fatty acids
HMG-CoA synthase	-104/-92	AGACCTtTGGCCC	Ketogenesis
L-fatty acid binding protein (L-FABP)	-68/-56	TGACCTaTGGCCT	Lipid transport
Adipocyte fatty acid binding protein (aP2)	-5222/-5209	TGAACTcTGATCC	Lipid transport
Malic enzyme	-328/-340	TCAACTtTGACCC	Fatty acid synthesis
Lipoprotein lipase	-169/-157	TGCCCTtTCCCCC	Hydrolysis of triglycerides
ApoA-I	-212/-197	TGACCCcTGCCCCT	Component of high densisty lipoprotein
ApoA-II	-734/-716	CAACCTtTACCCT	Component of high density lipoprotein

1.2.2 PPAR Structure

PPARs belong to the nuclear hormone receptor superfamily; their structure can be divided into six functional domains; A/B, C, D, E and F (Figure 1). Since no crystal structures of PPAR have been obtained, structural information is based on sequence similarities with nuclear receptors that have been crystalized. The A/B domain is the most poorly conserved domain among the isotypes and it is believed that this domain is involved in ligand-independent transactivation. The DNA-binding domain (DBD) or C domain is the most conserved region. This region contains two zinc fingers. At the carboxyl end of the first zinc finger are the 6 P-box aa that mediate DNA binding specificity. The D-box aa, which are located at the beginning of the second zinc finger, are involved in contacts between dimerized receptors. PPARs are unique in the fact that their D-box contains only 3 aa whereas other nuclear receptors have 5. The D domain contains the putative DBD carboxy-terminal extension and a hinge region that joins the C and E domains. The D domain is also believed to form an α-helical shape, which allows for binding and/or conformational changes. The E domain or ligand binding domain is the region that binds ligand, controls ligand-dependent transactivation and supplies the major dimerization interface. Once a ligand has bound, it is believed that the E domain undergoes a conformational change, specifically a shift in the position of helix 12. There are great sequence differences between PPAR isotypes in the E domain suggesting each subtype binds different ligands and subsequently performs different biological roles. Lastly, the F domain has no known biological function (Lemberger *et al.*, 1996, reviewed in Schoonjans *et al.*, 1996a).

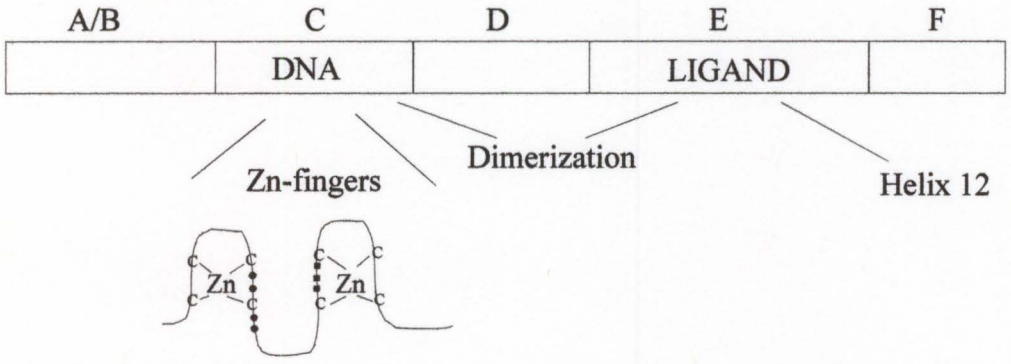

Figure 1: Functional domain structure of the nuclear hormone receptors. Modified from Schoonjans *et al.*, 1996a. The P-box amino acids are indicated by circles and the D-box amino acids are indicated by squares.

1.2.3 Activators/Ligands

Activators/ligands of PPARs have historically been referred to as peroxisome proliferators. Originally, peroxisome proliferators were characterized by the dramatic increase they caused in the size and number of peroxisomes in rats/mice livers (reviewed in Green, 1995). The earliest peroxisome proliferator discovered was clofibrate in 1963 (Paget 1963, Hess *et al.*, 1965). Since then, the list has grown to now include other hypolipidaemic drugs, fatty acids, herbicides, leukotriene antagonists, plasticizers and other synthetic compounds (Lock *et al.*, 1989, reviewed in Green, 1995). Research has now shown that peroxisome proliferators in fact activate PPARs which in turn increase the transcription of peroxisomal β-oxidation enzymes such as the acyl-CoA oxidase (AOx) enzyme (Marcus *et al.*, 1993, Varanasi *et al.*, 1996). There are several compounds that have been shown to be actual ligands for the PPAR isotypes. These include the natural occurring compound 15-deoxy-$\Delta^{12,14}$-prostaglandin J_2 and the synthetic compounds known as antidiabetic thiazolidinediones. Both of these ligands activate the PPARγ2 isoform and therefore lead to adipocyte differentiation (Forman *et al.*, 1995, Kliewer *et al.*, 1995, Lehman *et al.*, 1995). The peroxisome proliferators activate PPARα to the greatest extent. This finding correlates with the fact that PPARα is the isotype that is most prominently expressed in the liver. Originally, the only peroxisome proliferator found to be an actual ligand for PPAR was the synthetic compound Wy-14,643 (Devchand *et al.*, 1996). However, now several peroxisome proliferators have been identified as ligands for PPARs, these include fatty acids, eicosanoids and hypolipidemic agents (Krey *et al.*,

1997). Also, leukotriene B_4 (LTB_4), which recruits immune system cells to the site of an injury and thereby generates inflammation, has been found to be a natural ligand for PPARα. In addition, PPARα has been found to aid in the degradation of LTB_4 (Devchand *et al.*, 1996). The interaction between LTB_4 and PPARα appears to provide a feedback mechanism of down regulation for the inflammatory response.

1.2.4 Binding of PPARs to DNA

Nuclear hormone receptors (NHRs) recognize and bind to specific target sequences. The sequence recognized by PPARs is known as a peroxisome proliferator-responsive element (PPRE) and the corresponding DNA consensus sequence is TGACCT (refer to Table 1). NHRs bind as dimers and consequently two copies of the motif are required. The actual sequence, relative orientation and spacing between the two motifs renders specificity in a number of different ways (reviewed in Lemberger *et al.*, 1996). These include which nuclear receptor(s) will be able to bind to the element and with what affinity, the orientation of the nuclear receptors on the element and which partner, if not both, will be responsive to ligand. PPARs do not bind as monomers or homodimers but rather require the retinoid X receptor (RXR) for binding as a heterodimer (Miyata *et al.*, 1994). RXR also belongs to the hormone nuclear receptor superfamily and the natural occurring ligand for RXR is 9-*cis* retinoic acid (RA; reviewed in Mangelsdorf *et al.*, 1995). RXR has several different partners including itself, RAR (retinoid acid receptor) and LXR (liver X receptor; Miyata *et al.*, 1996) and can bind to several different target sequences depending on its partner (reviewed in Mangelsdorf *et al.*, 1995).

The first PPRE was discovered in the promoter of the AOx gene (Dreyer *et al.*,

1992, Tugwood *et al.*, 1992). Since then, PPREs have been found in several promoters including the rat mitochondrial 3-hydroxy-3-methylglutaryl-CoA synthase (mtHMG-CoAS) gene promoter (Rodríguez *et al.*, 1994).

1.3 Coactivators/Corepressors

Recently, several proteins have been identified that interact with both nuclear hormone receptors and basal transcriptional machinery. Consequently, these proteins add another regulatory element for transcription. Some of these proteins have been shown to act as transcriptional activators (coactivators), while others seem to inhibit the activation provided by the nuclear receptors (corepressors) (Glass *et al.*, 1997, reviewed in Shibata *et al.*, 1997). Some of the coactivators include p300/CBP (CREB-binding protein; Kamei *et al.*, 1996, Dowell *et al.*, 1997a), SCR-1 (steroid receptor coactivator-1; Oñate *et al.*, 1995), RIP140 (receptor-interacting protein 140; Cavaillès *et al.*, 1995), TIF2 (transcriptional intermediary factor; Voegel *et al.*, 1996)/GRIP1 (glucocorticoid receptor-interacting protein; Hong *et al.*, 1996), p/CIP (p300/CBP/co-intergrator-associated protein; Torchia *et al.*, 1997), P/CAF (p300/CBP-associated factor; Yang *et al.*, 1996, Korzus *et al.*, 1998) and PBP (PPAR-binding protein; Zhu *et al.*, 1997). Several of these coactivators such as SRC-1, p300, RIP140, and PBP have been shown to bind to and modulate transcription by PPAR (Zhu *et al.*, 1996, Dowell *et al.*, 1997a, Zhu *et al.*, 1997, Miyata *et al.*, 1998).

It is believed that coactivators bind to and stabilize the ligand binding domain of nuclear hormone receptors, specifically interacting with helix 12 and thereby releasing

corepressors (Wurtz *et al.*, 1996). Evidence also points to coactivator binding only in the presence of ligand (reviewed in Shibata *et al.*, 1997). Once ligand has bound to the receptor, this generally leads to a conformational change in the receptor and subsequently allows the coactivator to bind. Minimal, if any, interaction is usually detected between a coactivator and its receptor in the absence of ligand. However, this does not seem to be the case for all receptors. PPAR has been shown to interact in the absence of ligand with coactivators including p300 (with PPARα) and SRC-1 (with PPARγ) (Zhu *et al.*, 1996, Dowell *et al.*, 1997). Also, it seems that for PPARα and the coactivator RIP140 binding occurs in the absence of ligand and is not even enhanced upon ligand binding (Miyata *et al.*, 1998). Nonetheless, it has been shown that some form of conformation change does occur in PPARα upon exposure to ligand (Dowell *et al.*, 1997b) but the exact nature of this conformational change has yet to be elucidated.

Recently, it has been shown that many coactivators are able to interact with their corresponding receptor due to the presence of at least one specific motif; the LXXLL motif where L represents the aa leucine and X any aa. Mutations in this motif appears to result in a reduction or total abolishment of an interaction between the receptor and its coactivator. Also, by mutating the motif such that a receptor/coactivator interaction is lost, transactivation, as seen in transient transfection assays, is reduced to below basal levels (Heery *et al.*, 1997).

The main corepressors are N-CoR (nuclear receptor corepressor; Hörlein *et al.*, 1995) and SMRT (silencing mediator (corepressor) for retinoid and thyroid-hormone

receptors; Chen and Evans 1995). Corepressors are proteins that have been shown to interact with RXR/RAR or RXR/TR (thyroid-hormone receptor) heterodimers in the absence of ligand (Chen and Evans, 1995, Hörlein *et al.*, 1995). As the name corepressor implies, transactivation is inhibited when either SMRT or N-CoR is bound. It is believed that only once ligand has bound to the receptor that the resulting conformational change leads to the release of the corepressor, thereby allowing coactivators to form a new complex with PPAR and aid in transcriptional activation (reviewed in Shibata *et al.*, 1997).

1.4 Link Between PPARα and Mitochondrial HMG-CoAS

As mentioned previously, PPARα is involved in regulating both lipid metabolism and ketogenesis. Specifically, this is achieved through PPREs located upstream of genes encoding enzymes involved in both β–oxidation of fatty acids such as the AOx enzyme, and ketogenesis like mitochondrial HMG-CoAS. The mtHMG-CoAS enzyme provides one of the key regulatory points for ketogenesis. Ketogenesis provides an alternative source for fuel for the body during times of starvation, prolonged exercise or diabetes.

1.5 HMG-CoAS

1.5.1 HMG PPRE

The HMG PPRE was the first PPRE to be identified in a gene coding for a mitochondrial protein. The PPRE was identified to be 104 bp upstream of the rat mtHMG-CoAS gene. This PPRE is an imperfect direct repeat, AGACCT T TGGCCC, with one nucleotide separating each motif (DR1). This element was shown to bind

mPPARα and human RXRα as a heterodimer *in vitro* and be responsive to mPPARα and its activators, peroxisome proliferators, clofibrate, linoleic acid and monounsaturated oleic acid, in a dose dependent manner, in HepG2 cells (Rodríguez *et al.*, 1994). Since 1994, the HMG promoter has been found to be regulated by other nuclear receptors including COUP-TF, chicken ovalbumin upstream-promoter transcription factor, (Rodríguez *et al.*, 1997) and HNF-4, hepatocyte nuclear factor 4 (Rodríguez *et al.*, 1998).

1.5.2 General Properties

In mammals, HMG-CoAS is encoded by two different genes and in humans, the genes are on different chromosomes. One gene encodes the mitochondrial form while the other encodes the cytosolic form (cHMG-CoAS; reviewed in Hegardt, 1995). Each synthase performs a different metabolic role due to its different location within the cell. The mitochondrial form performs the first reaction in ketogenesis while the cHMG-CoAS is involved in the second step in cholesterol biosynthesis.

The cytoplasmic HMG-CoAS is 520 aa, has an apparent molecular weight of 53 kDa and has been found to be expressed ubiquitously (Clinkenbeard *et al.*, 1975b, Gil *et al.*, 1986). On the other hand, mtHMG-CoAS is 508 aa, has a molecular weight of 57 kDa and is present mainly in the liver (Clinkenbeard *et al.*, 1975a,b, Mascaró *et al.*, 1994). The two synthase enzymes behave as homodimers (Reed *et al.*, 1974) and have 66% identity in humans (Boukaftane *et al.*, 1994). High conservation occurs at the amino terminus and decreases as one moves toward the carboxyl terminus which supports the

notion of the two forms arising from a common ancestor or through a duplication event (Boukaftane *et al.*, 1994). The mtHMG-CoAS also contains, at the amino terminus, an additional 37 aa not found in cHMG-CoAS and this 37 aa is believed to be the mitochondrial targeting sequence (reviewed in Hegardt, 1995). The two types differ immunologically (Reed *et al.*, 1974) since antibodies have been made specific to each isotype. They also have different isoelectric points, a calculated 8.18 for human mtHMG-CoAS and 4.99 for cHMG-CoAS. Lastly, the two isotypes differ in their response to magnesium (Reed *et al.*, 1975a,b, Clinkenbeard *et al.*, 1974).

1.5.3 Metabolic Role

Hepatic ketogenesis provides lipid derived energy during carbohydrate deprivation for the brain, heart, kidney and other organs (reviewed in McGarry and Foster, 1980). The brain, unlike most organs, cannot utilize fatty acids, a noncarbohydrate energy source, for fuel. Consequently, ketogenesis becomes extremely important for this organ. Carbohydrate deprivation occurs during periods of starvation, sustained exercise or diabetes. Fat feeding also increases ketogenesis, which can be explained by the activation of PPAR, which in turn activates transcription of the mtHMG-CoAS gene via its own PPRE.

One known site of ketogenic control involves the two carnitine palmitoyl transferase enzymes and an acylcarnitine translocase reviewed in Guzmán and Geelen, 1992). These enzymes together regulate the entry of long-chain fatty acyl-CoA units into the mitochondria. The mitochondrial HMG-CoAS enzyme provides an additional two

mechanisms for control. One is succinylation (inactive enzyme) versus desuccinylation (active enzyme) of the protein. Another is the amount of mtHMG-CoAS mRNA that is produced, which is controlled, in part, by the PPRE in the promoter of the mtHMG-CoAS gene.

Cholesterol homeostasis, on the other hand, is maintained through feedback regulation involving two different mechanisms; receptor-mediated endocytosis of low density lipoproteins (LDL) or *de novo* synthesis which is regulated by HMG-CoA reductase (reviewed in Goldstein and Brown 1984). When cellular cholesterol is elevated, synthesis of LDL receptors, which bring cholesterol into the cell by receptor-mediated endocytosis, and *de novo* synthesis of cholesterol decreases. Conversely, when cellular cholesterol levels drop, the synthesis of LDL receptors and *de novo* cholesterol rise. When regulation of these two mechanisms is lost, an imbalance of the levels of LDL receptors and cholesterol can lead to hypercholesterolemia and athlerosclerosis (reviewed in Goldstein and Brown, 1977). HMG-CoA reductase is the major rate-controlling step in cholesterol biosynthesis since the activity of this enzyme exhibits the most profound changes in response to cholesterol levels. However, cHMG-CoAS, which provides the substrate for reductase, may also play an important step since it is also regulated by cholesterol levels.

1.5.4 Enzymatic Properties of HMG-CoAS

Both mitochondrial and cytoplamsic enzymes perform the same catalytic reaction, the condensation of acetyl-CoA and acetoacetyl-CoA to form HMG-CoA and free CoA (reviewed in Hegardt, 1995). Consequently, they also have very conserved active sites,

both containing a Cys residue, Cys^{129} in cHMG-CoAS and Cys^{166} in mtHMG-CoAS. This residue has been shown to be required for enzyme acetylation by acetyl-CoA (Rokosz *et al.*, 1994).

In the mitochondria, HMG-CoA is converted into acetoacetate by HMG-CoA lyase (refer to Figure 2). Acetoacetate is then broken down into D-3-hydroxybutyrate by 3-hydroxybutyrate dehydrogenase and acetone by aceto-acetate decarboxylase. Both D-3-hydroxybutyrate and acetone are known as ketone bodies. Conversely, in the cytoplasm, HMG-CoA is the substrate for HMG-CoA reductase, which produces mevalonate and thus initiates the isoprenoid pathway. This pathway produces cholesterol, dolichol, isopentyl adenosine, ubiquione and farnesylated proteins as end products (reviewed by Hegardt, 1995).

1.5.5 Inhibitors

Since mtHMG-CoAS is believed to be such a key control point in ketogenesis, much work has gone into designing inhibitors of this enzyme for research and medical purposes. There are only a few known specific inhibitors for the mitochondrial/cytoplasmic synthase enzymes. One of the main ones, F-244 a.k.a. 1233A and L-659,699, is a fungal β-lactone (Tomodo *et al.*, 1987). F-244 exerts similar effects on both rat synthases *in vitro* with an IC_{50} (50% inhibition concentration) of 0.12 μM for the partially purified cytoplasmic synthase and 0.8 μM for the partially purified mitochondrial form (Greenspan *et al.*, 1987). F-244 is also a specific inhibitor for the

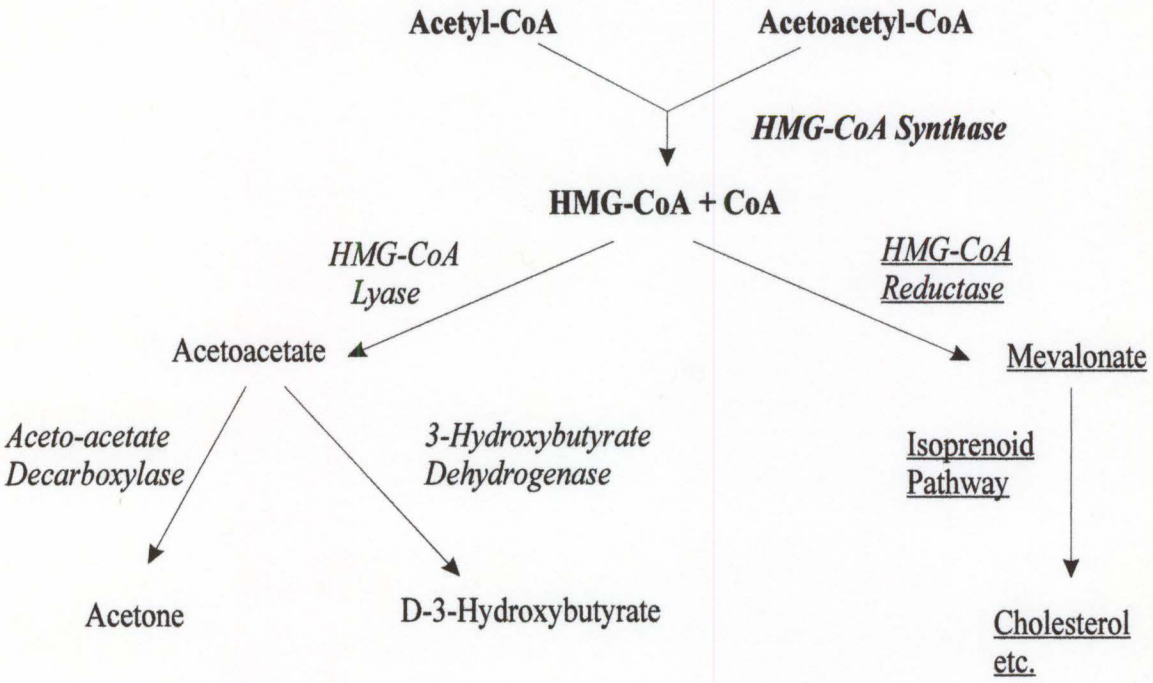

Figure 2: HMG-CoA synthase pathway in both the mitochondria and cytoplasm. The font in bold represents the common catalytic reaction catalyzed by HMG-CoA synthase. The names of the enzymes are in italics. The mitochondrial pathway is in regular font while the cytoplasmic pathway is in regular font and underlined.

synthase; little or no effect has been seen with F-244 on acetoacetyl-CoA thiolase, HMG-CoA reductase or fatty acid synthase (Greenspan *et al.*, 1987, Nagashima *et al.*, 1993). It has been shown that inhibition occurs through covalent interaction of the inhibitor with the enzyme (Mayer *et al.*, 1990). The interaction occurs between the inhibitor and a Cys residue in the active site (Rokosz *et al.*, 1994).

Inhibition has been shown to occur *in vitro* with purified enzyme and in cultured HepG2 cells and *in vivo* with animals (Greenspan *et al.*, 1987, 1993). The reversibility of the inhibition is still under debate and preliminary evidence suggests that the inhibition may be competitive with both substrates (Greenspan *et al.*, 1987, 1993).

1.6 Summary

PPARα is a nuclear hormone receptor that is involved in maintaining homeostasis though transcriptional regulation. PPARα binds as a heterodimer to RXRα, in conjunction with other regulatory proteins, on enhancer elements, PPREs, located upstream of target genes. Many of these target genes are proteins involved in lipid and fatty acid metabolism. One of these target genes is mtHMG-CoAS, a key regulatory protein involved in ketogenesis which provides lipid-derived energy for several organs during starvation and diabetes.

1.7 Project Overview

A potential interaction between mtHMG-CoAS and mPPARα was initially detected through a yeast dihybrid screen. Initially, the question of the importance and relevance of a mitochondrial protein interacting with a nuclear receptor was asked.

However, ketogenesis and more specifically mtHMG-CoAS is indeed regulated by PPARα and consequently an interaction between these two proteins would provide an interesting mode of autoregulation. Therefore, this interaction was studied further.

The characterization of the interaction between mtHMG-CoAS and mPPARα was done with the use of several different assays. Briefly, the *in vivo* interaction in yeast was reproduced with the use of solid phase capture and co-immunoprecipitation assays. Localization of the region in mtHMG-CoAS responsible for the interaction was performed with the construction of a site-directed mutant and a co-immunoprecipitation assay. The site-directed mutant demonstrated the importance of a LXXLL motif, in mtHMG-CoAS, for the interaction between mtHMG-CoAS and mPPARα. Transient transfection studies showed mtHMG-CoAS modulating mPPARα activity in a PPRE dependent manner. Lastly, under certain conditions, the cellular localization of mtHMG-CoAS, which was monitored by following hemagglutinin (HA) epitope tagged constructs, showed mtHMG-CoAS residing in both the mitochondria and the nucleus.

The mitochondrial HMG-CoAS enzyme is capable of interacting with mPPARα, it can modify mPPARα mediated transactivation and it can be localized to the nucleus. Consequently, the work presented here uncovers a new and exciting mode of gene regulation.

CHAPTER TWO

MATERIALS AND METHODS

2.1 Materials

2.1.1 Chemicals and Reagents

This list contains the specialized reagents that were utilized in this research and the companies that they were obtained from.

ampicillin	Sigma Chemical Company
bovine serum albumin	Pharmacia Biotech
charcoal, Dextran coated	Sigma Chemical Company
chloramphenicol	Sigma Chemical Company
coenzyme A	Sigma Chemical Company
deoxynucleotide triphosphates (dNTPs)	Pharmacia Biotech
goat anti-mouse Texas Red conjugated antibody	Jackson ImmunoResearch Laboratories
isopropyl-β-D-thiogalactoside (IPTG)	Biochemica and Synthetica
L-glutamine	Life Technologies
luciferin	Biosynth
molecular weight standards	

50 bp DNA ladder	Life Technologies
1 Kb DNA ladder	Life Technologies
low range SDS-PAGE standards	Bio-Rad
high range SDS-PAGE standards	Bio-Rad
mouse monoclonal anti-HA antibody	Boehringer Mannheim
penicillin (5,000U/ml)/streptomycin (5,000μg/ml)	Life Technologies
phenylmethylsulphonylfluoride (PMSF)	Boehringer Mannheim
p-phenylenediamine	Sigma
Protease Inhibitor Cocktail Tablets	Boehringer Mannheim
5X Reporter Lysis Buffer	Promega
9-*cis* retinoic acid	Sigma
salmon sperm DNA	Sigma Chemical Company
serum, calf	Life Technologies
serum, fetal bovine	Sigma Chemical Company
serum, goat	Life Technologies
sheep anti-mouse Ig, horseradish peroxidase	Amersham Life Science
trypsin-EDTA	Life Technologies
Wy-14,643	ChemSyn Laboratories

2.1.2 Radiochemicals

L-[^{35}S]-methionine (1151 Ci/mmol; 10μCi/μl)	NEN Life Science Products
[α-^{32}P]dATP (3,000 Ci/mmol; 10 μCi/μl)	Amersham Canada Ltd.

[^{14}C]-labelled molecular weight markers	Life Technologies

2.1.3 Cloning/Eukaryotic Expression Vectors

pSG5 (eukaryotic expression vector)	Stratagene
pGEX2T (bacterial expression vector)	Pharmacia Biotech
pGEX2TK (bacterial expression vector)	Pharmacia Biotech
pGEM5Zf(+) (bacterial expression vector)	Promega

2.1.4 Mammalian Cell Lines

BSC40s (African Green Monkey Kidney Cells derived from the BSC-1 line (Brockman and Nathans, 1974); cells are from The Massachusetts Institute of Technology (MIT))
Cos-1 (African Green Monkey Kidney Cells transformed with the SV40 T Antigen (Gluzman, 1981); cells are from the American Type Culture Collection (ATCC))

2.1.5 Oligonucleotides

The oligonucleotides described in Table 1 were used for DNA sequencing, vector construction and PCR amplification. All oligonucleotides were obtained from either The Central Facility of the Institute for Molecular Biology and Biotechnology, McMaster University or Dalton Chemical Laboratories Inc.

Table 2: Oligonucleotides

Oligo-Nucleotide	Sequence	Purpose
AB3369	5'GGCCTACCCATACGACGTCCCAGACTACGCTTAGC3'	HA-epitope Tag (for)
AB3370	3'CGCCGGATGGGTATGCTGCAGGGTCTGATGCGAAT5'	HA-epitope Tag (rev)
AB4950	5'GATCCTTTCCCGAACGTGACCTTTGTCCTGGTCCCCTTTTGCT3'	AOx PPRE (for)
AB4951	3'GAAAGGGCTTGCACTGGAAACAGGACCAGGGGAAAACGATCTAG5'	AOx PPRE (rev)
AB8959	5'GATCCTGACTTGTTCTGAGACCTTTGGCCCAGTTTTTCTGAGGCAGGCAGAGGA3'	HMG-CoAS PPRE (for)
AB8960	3'GACTGAACAAGACTCTGGAAACCGGGTCAAAAAGACTCCGTCCGTCTCCTCTAG5'	HMG-CoAS PPRE (rev)
AB1118	5'TAATACGACTGCACTATAGGG3'	T7 promoter primer
AB5597	5'GATTTAGGTGACACTATAG3'	SP6 promoter primer
AB8660	5'GCGCGGATCCAGAATTCGGCATGCCTGGGTCACTT3'	PCR cHMG-CoAS (for)
AB8661	3'CCCACATTTCGAAGTGTCTAGATCCTAGGCTTAAGGGCC5'	PCR cHMG-CoAS (rev)
AB11634	5'GGTGCCTGGCCTCGGTTCTGTCCCACC3'	PCR L393V mtHMG-CoAS (for)
AB11635	3'CCACGGACCGGAGCCAAGACAGGGTGG5'	PCR L393V mtHMG-CoAS (rev)
AB11636	5'CCTCTCCACTCACAATGGG3'	Sequence L393V mtHMG-CoAS/PCR SacII site mtHMG-CoAS (for)
AB11828	3'ATACGGGCCGCAGGGCAGTGGCGCCATTCGATCGCC5'	PCR SacII site mtHMG-CoAS (rev)
AB12444	5'TTAAAAATATGATTCACG3'	Sequence SacII site mtHMG-CoAS
AB9972	5'GAGCAAAGGAAG3'	Sequence CPS LUC

2.1.6 Plasmids

2.1.6.1 Commercial Vectors

pSG5 (Stratagene): an ampicillin resistant eukaryotic expression vector containing a SV40 early promoter and a SV40 poly-A signal. pSG5 also contains a T7 promoter upstream of the multiple cloning site (MCS).

pGEX-2T (Pharmacia Biotech): an ampicillin resistant bacterial expression plasmid containing a tac promoter, a lac operon and a coding region for thrombin cleavage upstream of the GST gene. The MCS is located directly downstream of the GST cDNA.

pGEX-2TK (Pharmacia Biotech): pGEX-2TK is identical to pGEX-2T except for the additional feature of containing a kinase recognition site just downstream of the thrombin cleavage coding region.

pGEM5Zf(+) (Promega): an ampicillin resistant plasmid containing both a T7 and SP6 promoter flanking either end of the MCS.

2.1.6.2 Constructed by Others

pCPS-Luc (Zhang *et al.*, 1992): a luciferase expression vector containing the minimal promoter for the gene encoding rat liver carbamyl-phosphate synthetase (CPS).

pCAN-HA: pcDNA3, which is available from Invitrogen, was modified (John Hassell, McMaster University) to contain HA tags in three different reading frames (pCAN-HA1-3) within the MCS. pCAN-HA, like pcDNA3, is ampicillin resistant and contains both a T7 and SP6 which flank opposite ends of the MCS. This vector also contains the human

cytomegalovirus early promoter and SV40 ori. The HA tag was cloned between the NcoI and BamHI sites within the MCS.

pHSH-1: a generous gift donated to us from Boukaftane *et al.*, 1994, contains the carboxy terminal cDNA of human mtHMG-CoAS starting at aa 144.

pSG5-mPPARα: pSG5 containing full length mPPARα that was cloned into the BamHI site.

pSG5-RXRα: pSG5 containing full length human RXRα that was cloned into the EcoRI site.

pGEX-2T-RXRα: pGEX-2T containing full length human RXRα that was cloned downstream and in frame of the GST gene in the EcoRI site. Initially, the EcoRI site in pGEX-2T was made into blunt ends using the Klenow fragment of DNA Polymerase. Then the RXRα fragment, removed from the BglII site in pGEM7Zf(+)-RXRα, had its ends made blunt using Klenow. The blunt RXRα fragment was then cloned into the blunt vector (pGEX-2T).

pGEM5Zf(+)-cHMG-CoAS: a generous gift from Gil *et al.*, 1996 and contains the full length hamster cHMG-CoAS

pCPS-Luc-1X HMG PPRE: pCPS-Luc vector containing 1 copy of the HMG PPRE in the forward orientation within the BamHI site using annealed oligos AB8959 and AB8960 that possess BamHI/BglII ends.

pCPS-Luc-2X AOx PPRE (Marcus *et al.*, 1993): pCPS-Luc vector containing 2 copies of the AOx PPRE in an indirect repeat (→←).

2.1.6.3 Constructed During Project

pHSH-2: pHSH-2 is only different from pHSH-1 in that it contains the full length human mtHMG-CoAS. The amino terminus of human mtHMG-CoAS (aa 1-345), pulled from the yeast dihybrid screen, was cloned from pGAD10 (yeast dihybrid vector) using XhoI and NdeI and cloned into the same sites in pHSH-1 to yield a full length cDNA of human mtHMG-CoAS.

pSG5-mtHMG-CoAS: full length human mtHMG-CoAS was cloned into the EcoRI site in pSG5 from the EcoRI site in pHSH-2.

pSG5-cHMG-CoAS: full length hamster cHMG-CoAS was cloned into the BamHI site in pSG5 from the BamHI ends, created by PCR, located at both termini of cHMG-CoAS. The BamHI ends, created by PCR, were done using oligos AB8660 and AB8661 in conjunction with the template, pGEM5Zf(+)-cHMG-CoAS.

pGEX-2TK-mPPARα: full length mPPARα was digested with BamHI from pSG5-mPPARα and cloned, downstream and in frame of the GST start codon, in the BamHI site.

pCPS-Luc-2X HMG PPRE: was constructed from pCPS-Luc-1X HMG PPRE using oligos AB8959 and AB8960 that contain BamHI /BglII ends. The annealed oligos were cloned into the BamHI site of pCPS-Luc-1X HMG PPRE, the second copy formed a direct repeat of the synthase PPRE (→→) which was confirmed by sequencing using oligo AB9972.

pCAN-HA-mtHMG-CoAS: full length human mtHMG-CoAS was digested with EcoRI from pSG5-mtHMG-CoAS and cloned into the EcoRI site downstream and in frame of the HA start codon.

pCAN-HA-cHMG-CoAS: full length hamster cHMG-CoAS was digested with BamHI from pSG5-cHMG-CoAS and cloned into the BamHI site downstream and in frame of the HA start codon.

pCAN-HA$^-$: The HA tag was removed from pCAN-HA by digesting with BamHI and HindIII. The vector ends were made blunt using Klenow and then the vector ends were religated.

pCAN-mtHMG-CoAS-HA: The first step in making this construct involved cloning mtHMG-CoAS into the EcoRI site in pCAN-HA$^-$ from the same site in pSG5-mtHMG-CoAS. A new site (SacII) was then created by PCR right before the stop codon in mtHMG-CoAS using oligos AB11636 and AB11828. The new PCR carboxy end of mtHMG-CoAS was then digested with BsrGI and NheI and cloned into the same sites in mtHMG-CoAS in pCAN-HA$^-$. HA oligos (AB3369 and AB3370) with the SacII ends were then cloned into the new SacII site in mtHMG-CoAS. Potential clones were screened by sequencing with oligo AB12444 to ensure insertion of the HA tag in the correct orientation.

pCAN-HA-mtHMG-CoAS-HA: pCAN-mtHMG-CoAS-HA was digested with BsrGI and NheI which released the carboxy end of mtHMG-CoAS with the HA tag and this fragment was then cloned into the same sites in pCAN-HA-mtHMG-CoAS.

pSG5-mtHMG-CoAS (L393V): The QuickChange™ Site-Directed Mutagenesis Kit from Stratagene and oligos AB1634 and AB1635 were used to change aa 393 in pSG5-mtHMG-CoAS from a leucine to a valine to create pSG5-mtHMG-CoAS (L393V). Potential clones were screened by dideoxy sequencing with oligo AB1636 to ensure that the clone had the correct aa change.

pCAN-mtHMG-CoAS (L393V)-HA: pSG5-mtHMG-CoAS (L393V) was digested with HindIII and KpnI to release the carboxyl end of mtHMG-CoAS containing the L393V mutation and this fragment was then cloned into the same sites in pCAN-mtHMG-CoAS-HA. Potential clones were sequenced to determine if they contained the L393V mutation. Sequencing was performed with oligo AB11636.

pCAN-HA-mtHMG-CoAS (L393V)-HA: pCAN-mtHMG-CoAS (L393V)-HA was digested with BsrGI and NheI to release the carboxy end of mtHMG-CoAS containing both the mutation and the carboxy HA tag. This fragment was then cloned into the same sites in pCAN-HA-mtHMG-CoAS.

2.2 Methods

2.2.1 Plasmid Construction

All plasmid construction and manipulation was carried out using standard procedures as outlined in Ausubel *et al.*, 1998.

2.2.2 Small Scale Plasmid DNA Purification

Two methods were utilized for the purification of plasmid DNA, a small scale "miniprep" method and a large scale column purification.

The small scale preparation was performed by utilizing a lysis by boiling method (Sambrook *et al.*, 1989). The procedure involved the pelleting of 1.5 ml of a 37°C overnight bacterial culture that was grown in 5 ml of 2YT (15 g bactotryptone, 10 g yeast extract, 5 g NaCl in 1 L water) supplemented with ampicillin to a final concentration of 100 μg/ml. The pellet was resuspended in 350 μl of STET buffer (0.1 M NaCl, 10 mM Tris-HCl (pH 8.0), 1 mM EDTA (pH 8.0) and 5% Triton X-100) and 30 μl fresh lysozyme (10 mg/ml in 10 mM Tris-HCl (pH 8.0)). The sample was then boiled for 40 secs and centrifuged for 10 mins to pellet the cell debris. Removal of the debris was done with a sterile toothpick. 200μl of NH_4Ac and 700μl of isopropanol was then added to the supernatant. The resulting solution was then flash frozen in liquid nitrogen and spun at 14,000 rpm at 4°C for 10 mins. The resulting DNA pellet was subsequently washed with 70% ethanol. DNA was then resuspended in TE (10 mM Tris-HCl (pH 8.0), 1 mM EDTA (pH 8.0)) containing RNAse A (100 μg/ml).

2.2.3 Large Scale Plasmid DNA Purification

The large scale method of DNA purification involved the use of DNA purification columns, available from Qiagen, and chloramphenicol amplification. For each plasmid,

one 50 ml flask of 2YT media containing ampicillin (100 μg/ml) was inoculated with a single colony. The culture was grown overnight at 37°C with shaking. The next day 25 ml of the overnight culture were added to 500 mL of 2YT media containing ampicillin (100 μg/ml). The subsequent culture was shaken and grown at 37°C to an OD600 of 0.5 upon which chloramphenicol was added to a final concentration of 34 mg/ml. The culture was again grown at 37°C overnight and harvested the following day. The culture was spun down at 4°C for 15 mins at 6,000 rpm and then resuspended in 10 ml buffer P1 (resuspension buffer; 50 mM Tris-HCl (pH 8.0), 10 mM EDTA (pH 8.0), 100 μg/ml RNase A). Buffer P2 (10 ml; lysis buffer; 200 mM NaOH, 1% SDS) was then added and the solution was incubated at room temperature for 5 mins. Chilled buffer P3 (neutralization buffer; 3.0 M KAc (pH 5.5)) was added and the solution was kept on ice for 20 mins. The cell debris was pelleted at 4°C for 30 mins at 16,000 rpm. Meanwhile, one Qiagen column was equilibrated with 10 ml of buffer QBT (750 mM NaCl, 50 mM MOPS (pH 7.0), 15% ethanol, 0.15% Triton X-100). The supernatant was then loaded and the flow through saved. The column was washed with 60 ml of buffer QC (1.0 M NaCl, 50 mM MOPS (pH 7.0), 15% ethanol) and eluted with 15 ml of buffer QF (1.25 M NaCl, 50 mM Tris-HCl (pH 8.5), 15% ethanol). The column was again equilibrated with 10 ml of buffer QBT and the second lysate was loaded, washed and eluted in the same manner. Plasmids were precipitated with 0.7 volumes of isopropanol and pelleted at 11,000 rpm. The pellets were washed twice with 70% ethanol and resuspended in sterile TE (pH 8.0). The DNA concentration was determined by fluorometry and the plasmid

concentration adjusted to 1 mg/ml.

2.2.4 DNA Quantification by Fluorometry

Plasmid concentration was quantified by fluorometry using the method outlined by Hoefer and a Hoefer Mini-Fluorometer (TKO 100). Calf thymus DNA, at a known concentration, was used as the standard. Plasmid DNA was diluted into 2 ml of the 1X TNE buffer (1 mg/ml Hoescht 33258 dye, 0.2 M NaCl, 10 mM Tris-HCl, 1mM EDTA (pH 7.4)). The sample was measured in a cuvette and the concentration was adjusted to 1 mg/ml.

2.2.5 Bacterial Transformation

DH10β cells were made competent by a modified RbCl method provided by Ausubel *et al.*, 1997. Generally, a 37°C overnight culture of the noncompetent cells (50 ml) in LB (no glucose, ampicillin (100 μg/ml)) was grown. The next day 200 ml of LB (no glucose, ampicillin (100 μg/ml)) was inoculated with the overnight culture. The subsequent culture was grown at 37°C until the OD600 reached 0.45. The culture was collected in 4 cold 50 ml sterile tubes and kept on ice for 10 mins. The culture was then spun at 4°C for 10 mins at 3,000 rpm. The supernatant was poured off and the pellets were gently resuspended each in 20 ml of ice cold RF1 buffer (100 mM RbCl, 50 mM $MnCl_2 \bullet 4H_20$, 30 mM KOAc, 10 mM $CaCl_2 \bullet 2H_20$, 15% glycerol, pH solution to 5.8 with acetic acid, filter sterilize). The cells were incubated for 1 hr on ice and then spun at 4°C

for 10 mins at 3,000 rpm. The supernatant was again poured off and the pellets were now redissolved in 8 ml ice cold RF2 buffer (10 mM MOPS, 10 mM RbCl, 75 mM $CaCl_2 \bullet 2H_20$, 15% glycerol, pH solution to 6.8 with NaOH, filter sterilize). The cells were aliquoted, 200 µl, into -70°C chilled sterile eppendorf tubes and stored at -70°C.

Once competent, 50 µl of cells were incubated on ice with 5-10 ng of DNA for 30 mins. DNA and cells were then heat shocked for 2 mins at 42°C and subsequently placed on ice again for 2 mins. 1 mL of 2YT was then added and the mixture was incubated at 37°C for 1 hr. After 1 hr, 100 µl of the solution was plated out on a 2YT plate containing ampicillin (100 µg/mL). The plate was then incubated at 37°C overnight.

2.2.6 Sequencing

Sequencing of DNA was performed using a dideoxy sequencing kit, ^{T7}Sequencing^{TM} Kit, from Pharmacia Biotech. Initially, the template DNA was denatured by mixing 16 µl of plasmid DNA (5 µg) with 1 µl of 4 M NaOH and 1 µl of 4 mM EDTA (pH 8.0) and incubating for 5 mins at room temperature. Then 2 µl of 2 M NH_4AC and 60 µl of ice cold ethanol was added. The mixture was then flash frozen in liquid nitrogen and spun at 4°C for 15 mins. The resulting pellet was washed twice in 70% ethanol, dried and redissolved in 20 µl water. The primer was annealed to the denatured template by incubating 10 µl of the template DNA (1.5 to 2 µg of DNA) with 2 µl of primer (1 to 2 pmol) and 2 µl of annealing buffer. The mixture was then incubated at 60°C for 10 mins and cooled at room temperature for 10 mins. The mixture was then added to 3 µl of

labeling mix and 1 µl of [α-^{32}P]dATP and 2 µl of ¼ diluted T7 DNA Polymerase. This labeling reaction was incubated at room temperature for 5 mins. After the labeling reaction was complete, 4.5 µl of this reaction was added to four pre-warmed tubes (37°C) each containing 2.5 µl of one of the four nucleotide mixes. This termination reaction occurred for 5 mins at 37°C. Following the termination reaction, 5 µl of the stop solution was added to each tube. The tubes were then heated at 75°C for 2 mins and loaded onto an 8% acrylamide sequencing gel prewarmed to 55°C. The sequencing gel was run at 80 watts for approximately 2.5 hrs, dried and exposed to Kodak X-ray film.

2.2.7 *In vitro* Transcription and Translation

In vitro transcription and translation reactions were carried out using the Promega uncoupled system. For the transcription reaction, plasmids (5 µl of 1 µg/µl) containing a T7/SP6 promoter were incubated with 10 µl 5X transcription buffer, 5 µl 100 mM DTT, 1.5 µl RNasin ribonuclease inhibitor (40 units/µl $\rightarrow$ 60 units), 2.5 µl 10 mM ATP, CTP and UTP, 2.5 µl 1 mM GTP, 5 µl 5 mM m^7G (5') ppp(5')G, 3 µl SP6/T7 RNA Polymerase (15 units/µl $\rightarrow$ 45 units) and 10.5 µl nuclease free water. The mixture was then incubated at 37°C for 2 hrs. After incubation, 130 µl of water and 20 µl of 3M NaAc were added to the mixture. The solution then underwent two PCI extractions (25:24:1 of phenol:chloroform:isoamyl alcohol) followed by three chloroform extractions. Ethanol (600 µl) was added to the solution that then was frozen in liquid nitrogen and spun down at 14,000 rpm for 15 mins. The resulting RNA pellet was washed twice in 70% ethanol

and redissolved in 25 µl water and 1 µl of RNasin ribonuclease inhibitor. The RNA solution was then aliquoted into microcentrifuge tubes (2 µl/tube) and stored at -70°C.

In vitro translation reactions were performed with 1 tube of RNA (from above)/50 µl translation reaction. To one tube containing 2 µl of RNA, 35 µl of rabbit nuclease treated lysate, 1 µl RNasin ribonuclease inhibitor (40 units/µl), 1 µl of 1 mM amino acid mixture (+/- methionine), 4 µl L-[^{35}S]-methionine (10 mCi/mL) (for radioactive translates only) and 7 µl water were added. The mixture was then incubated at 30°C for 1 hr and then stored at –70°C/run on a 10% SDS-PAGE gel, dried and exposed to Kodak X-ray film.

2.2.8 Polymerase Chain Reaction

The Polymerase Chain Reaction (PCR) was used for several different cloning strategies and was performed according to the guidelines outlined by Ausubel *et al.*, 1997. The general aspects of the reactions are as follows. A reaction mixture consisted of 10 µl 10X Thermophillic Buffer, containing 2 mM $MgSO_4$, (New England Biolabs), 0-6 µl of 100 mM $MgSO_4$ (gives 2 to 8 mM final $MgSO_4$ concentration), 10 µl of each 4 mM dNTP (final concentration of each is 1 mM), x µl of DNA (1-100 ng), 1 µl of each primer (1 µM/100 ρmol), 1 µl of Vent DNA Polymerase (2,000 U/ml → 2 U) and water to give a total reaction volume of 100 µl.

The cycling reactions are generally as follows. The first cycle consisted of 5 mins at 94°C, 1 min at 55°C (the annealing temperature is dependent upon the primers, to

calculate the rough annealing temperature: [(G+C) X 4°C + (T+A) X 2°C - 10°C]) and 2 mins (the extending time varies with the length of the PCR product, the general rule is 1 Kb/min) at 72°C. Subsequent cycles (around 30) were 1 min at 94°C, 1 min at 55°C and 2 min at 72°C. After the cycling reactions were completed, the samples were kept at 4°C until they could be analyzed by either a 1% agarose or a 4% NuSieve gel.

2.2.9 Electrophoretic Mobility Shift Assays

Electrophoretic mobility shift assays (EMSAs) were utilized to determine the binding of proteins to DNA binding sites. They were modified from the technique of Fried and Crothers, 1981.

The DNA probe was synthesized by annealing two oligos together; the two oligos were heated at 75°C for 10 mins and then slowly cooled (1°C/min) to below 30°C. The annealed DNA was then run on a 4% NuSieve gel, containing 0.5 μg/mL ethidium bromide, and the band was run from the gel onto NA45 paper. The paper was then heated in DEAE elution buffer (10 mM Tris-HCl (pH8.0), 1 mM EDTA (pH 8.0), 1 M NaCl) for 30 mins at 65°C. The paper was then removed and the mixture was spun down at 14,000 rpm for 2 mins to remove any gel debris. The supernatant was then removed and mixed with 8 μl $MgCl_2$ and 1 mL ethanol and spun down at 14,000 rpm at 4°C for 15 mins. The pellet was rinsed twice with 70% ethanol and resuspended in water to yield ~20 ρmol/μl. The probe was then synthesized by reacting 1 μl annealed and purified oligos, 2.5 μl of 10X Klenow buffer, 10 μl [α-^{32}P]dATP, 1 μl of 5 mM dCTP, dTTP, and dGTP, 8.5 μl

water and 1 µl Klenow at 25°C for 25 mins. After the 25 min incubation, 0.5 µl of 0.5 M EDTA and 75 µl of TE were added to the mixture. Passing the mixture through two Sephadex G-50 columns then purified the synthesized probe. A scintillation counter was then used to measure 1 µl of the synthesized probe.

The bandshift binding reaction was a mixture of *in vitro* translated non-radioactive proteins, 20 ρmol [α-^{32}P]dATP Klenow labeled DNA, 1 µl of 4 µg/µl polydIdC, 1 µl of 4 µg/µl bovine serum albumin (BSA), 1 µl of 4 µg/µl salmon sperm DNA, and 5 µl of Buffer C (20 mM HEPES-KOH, 25% glycerol, 420 mM NaCl, 1.5 mM $MgCl_2$, 0.2 mM EDTA, 0.5 mM DTT, 0.2 mM PMSF), for a total volume of 15 µl. The resulting mixture was incubated for 25 mins at 28°C. After incubation, 1 µl of bandshift loading buffer (0.25% bromophenol blue, 0.25% xylene cyanol FF, 30% glycerol in water) was added to each tube and the mixture was then loaded on a 4% non-denaturing acrylamide gel. The gel was then run at 240 volts, dried and exposed to Kodak X-ray film.

2.2.10 Overexpression and Purification of a Glutathione S-Transferase (GST) Binding Protein Fusion

A GST binding protein fusion of mPPARα was constructed by cloning mPPARα into pGEX-2TK (refer to plasmid section 2.1.2.3). Purification of the fusion plasmid was performed using a modified technique from that provided by Pharmacia Biotech. A 1L 2YT culture supplemented with ampicillin (100 µg/mL) of DH5α *E. coli* transformed with pGEX-2TK-mPPARα was grown at 37°C to an OD600 of 0.5. At this point IPTG

was added to a final concentration of 0.1 mM and the culture was grown for an additional 5 hrs. Cells were harvested by centrifugation, 8,000 rpm at 4°C, and resuspended to a total volume of 50 ml with PBS (260 mM NaCl, 10 mM Na_2HPO_4, 10 mM NaH_2PO_4). Cells were lysed using a probe sonicator for 8, 30 sec bursts with a 30 sec incubation on ice in between. Cell debris was spun out at 4°C by centrifugation at 10,000 rpm. The supernatant was loaded onto a disposable column containing a bed volume of 2 ml of glutathione Sepharose 4B beads (Pharmacia Biotech) that had been washed 3X with 10 column volumes of PBS. Once the cell lysate was loaded, the column was again washed 3X with 10 column volumes of PBS. Proteins were eluted off with the addition of 1 mL of glutathione elution buffer (10 mM reduced glutathione in 50 mM Tris-HCl (pH8.0)) per mL bed volume. The column was incubated at room temperature for 10 mins to elute the fusion protein. The eluant was then collected and elution of the protein was monitored by microtitre plate Bradford assay. Fractions were analyzed by a 10% SDS-PAGE gel and samples containing protein were pooled and dialyzed overnight into PBS containing 20% glycerol. Protein concentration was determined by Bradford analysis and the appropriate samples were stored at -20°C.

2.2.11 Solid Phase Capture Assay

Solid phase capture assays were performed using a modified technique from that provided by Pharmacia Biotech. Glutathione Sepharose 4B beads (Pharmacia Biotech) (100 µl) were washed 3X with PBS and made into a 50% slurry. GST fusion proteins

plus 500 µl PBS were then added to the beads (20 µl of 50% slurry) to obtain maximum saturation of the beads with fusion protein (50 µg/10 µl of 50% slurry of beads). Fusion protein and beads were incubated for 1 hr at 4°C. The beads were then washed 3X with 1 mL of PBS. Following the washes, the beads plus attached fusion protein were incubated with between 5-10 µl of *in vitro* translated L-[^{35}S]-methionine labeled protein and 500 µl of PBS/0.1% NP-40/2% BSA for 30 minutes at room temperature. The beads were then washed 3X in 1 mL of PBS/0.1% NP-40/2% BSA and 2X in 1 mL of PBS/0.05% NP-40/2% BSA. The beads were then pelleted at 1,000 rpm and boiled for 5 mins in 20 µl 2X SDS-PAGE loading buffer (100 mM Tris-HCl (pH6.8), 200 mM DTT, 4% SDS, 0.2% bromophenol blue, 20% glycerol). One half of the sample was then loaded onto a 10% SDS-PAGE gel, the gel was dried and exposed to Kodak X-ray film.

2.2.12 Immunoprecipitations

The procedure used for the immunoprecipitations was modified from the technique provided by Fujiki *et al.*, 1984. *In vitro* translated L-[^{35}S]-methionine labeled proteins were diluted with 9 volumes IP buffer (1% NP-40/10 mM Tris-HCl (pH 7.5)/150 mM NaCl/10 mM methionine/1/5 dilution of 7X stock of protease inhibitor cocktail). Diluted translations were spun at 41,000 rpm (100,000 gmax) at 4°C for 1 hr. The supernatant was removed and divided as needed, with the addition of SDS to 0.1% and EDTA (pH 7.5) to 2 mM. Diluted proteins were then incubated together for 90 mins at room temperature. Preimmune/immune serum was then added to each tube (5 µl (275 µg total

protein) of rabbit polyclonal anti-mPPARα, anti-RXRα or preimmune) and the mixture was again incubated for 90 mins at room temperature followed by incubation at 4°C overnight. The next day 20 µl of protein A conjugated agarose beads (Biorad; having been washed in PBS and made into a 50% slurry) were added to the tube and the mixture was incubated for 90 mins at room temperature. Following incubation the beads were washed 3X with 0.1% NP-40/10 mM Tris-HCl (pH 7.5)/150 mM NaCl/10 mM methionine and 2X with 0.05% NP-40/10 mM Tris-HCl (pH 7.5)/150 mM NaCl/10 mM methionine. The beads were then pelleted at 1,000 rpm, 20 µl of 2X SDS-PAGE buffer was added, the samples were boiled for 5 mins and half of the sample was loaded onto a 10% SDS-PAGE gel. The gel was then dried and exposed to Kodak X-ray film.

2.2.13 Site-Directed Mutagenesis

Mutagenesis was performed using the QuikChange™ Site-Directed Mutagenesis Kit from Stratagene. In general, the reaction mix contained 5 µl of 10X reaction buffer, 5-50 ng of dsDNA template, 125 ng of oligonucleotide primer #1 and 2, 1 µl of dNTP mix (10 mM final concentration of each), and water to a final volume of 50 µl. Then 1 µl of *Pfu* DNA Polymerase (2.5U/µl) was added. The reaction was then placed into the PCR machine (Techne, PHC-3) with the following cycling parameters: 1 cycle at 95°C for 30 secs, 12-18 cycles (12 cycles for a point mutation, 16 cycles for a single amino acid change and 18 cycles for multiple amino acid deletions or insertions) at 95°C for 30 secs, 55°C for 1 min and 68°C for 2 mins/kb of plasmid length. Following temperature cycling,

the reaction(s) were placed on ice for 2 minutes and then 1 µl of DpnI restriction enzyme (10 U/µl) was added to each amplification reaction. The reaction(s) were mixed by pipetting up and down several times and then incubated at 37°C for 1 hr to digest the parental supercoiled dsDNA. After digestion, 1 µl from each reaction was added to competent cells to do a bacterial transformation as outlined above. Individual colonies were chosen to screen by sequencing.

2.2.14 Transient Transfection Assays

Transient transfection assays were modified from the protocol of Graham and Van Der Eb, 1973. The first step was to mix plasmid DNA (total of 20 µg), ssDNA (used as filler at 1 mg/mL) and water. Immediately before the addition of 2X HBSS (0.28 M NaCl, 50 mM HEPES, 1.5 mM $Na_2HPO_4 \bullet 7H_20$, pH solution to 7.2 with NaOH, filter sterilized), 2M $CaCl_2$ (filter sterilized) was added to bring the [mM] of $CaCl_2$ to 0.25 mM. To this solution was added an equal volume of 2X HBSS while vortexing gently. The solution was then incubated at room temperature for 20 mins at which time 240 µl of precipitate was added to each well of the 6 well plate. The cells in each well were plated the day before using 2.0×10^5 cells/well. The precipitate was incubated on the cells for 16 hrs at which time the cells were washed with PBS and fresh media was added. The cells were harvested at 24 hrs after washing with PBS. To harvest the cells, 300 µl of 5X reporter lysis buffer was added to each well. The cells were immediately scraped off the plate with a cell lifter and collected in microfuge tubes. Each tube was vortexed at a high speed for

10 secs and then spun down for 10 seconds at room temperature to pellet the cell debris. The supernatant was then collected and put into a fresh microfuge tube. The lysates were kept on ice until assayed.

2.2.15 Luciferase Assay

Since the reporter gene used in the transient transfection assays was luciferase, the cell extracts were assayed for luciferase activity by utilizing a modified protocol from Promega. The assay consisted of mixing 10 µl of lysate with 100 µl of assay buffer (470 µM luciferin, 270 µM coenzyme A, 530 µM ATP, 33.3 mM DTT, 20 mM Tricine, 1.07 mM $(MgCO_3)_4Mg(OH)_2 \bullet 5H_2O$, 2.67 mM $MgSO_4$, 0.1 mM EDTA). The mixing of lysate and assay buffer was performed by a Lumat LB 9507 luminometer that measured relative light units (R.L.U.). Protein content was also measured using the Bradford Assay from Biorad and the R.L.U. values were adjusted accordingly. Each graph consists of the combined data from two experiments each done in duplicate. The standard deviation was combined from each experiment using the following forumula:

$[((n_1-1)s_1^2 + (n_2-1)s_2^2)/(n_1+n_2-2)]^{1/2}$

where n = the sample number, s = the standard deviation

2.2.16 Western Blotting

Cos-1 cells were transfected (as described previously) with 1.25 µg plasmid/well and harvested in 200 µl RIPA buffer (10% NP-40, 0.4% DOC, 66 mM EDTA (pH 7.4), 10 mM Tris-HCl (pH 7.4), 1 mM PMSF)/well. Protein content was determined by the Biorad protein assay and BSA was used to create the standard curve. Proteins (75 µg)

were loaded onto a 10% SDS-PAGE gel and transferred onto Hybond nitrocellulose (Amersham Life Science) at 30 volts overnight in 1X transfer buffer (20 mM Tris Base, 0.16 M glycine, 20% methanol). The western blot procedure was a modified version from the one provided by Amersham Life Science. The nitrocellulose was blocked in 5% skim milk powder in TBST (20 mM Tris-HCl (pH 7.5), 150 mM NaCl, 0.05% Tween 20) followed by one 15 min wash and two 5 min washes in TBST. The blot was then incubated with the primary antibody, mouse monoclonal anti-HA, at a concentration of 5 μg/mL in 1% skim milk in TBST for 1 hr. The nitrocellulose was then washed as before and then incubated with the secondary antibody, sheep anti-mouse Ig horseradish peroxidase, at a 1/1000 dilution in 1% skim milk in TBST for 1 hr. The blot was then washed as above and incubated with the detection solution (ECL detection assay from Amersham Life Science) for 1 min which resulted in chemiluminescence. The nitrocellulose was then blotted dry and exposed to Reflection™ film for 1-5 mins.

2.2.17 Immunofluorescence

Immunofluorescence was performed, with a few changes, according to the method outlined by Ausubel *et al.*, 1997. Cos-1 cells were transfected (as described above) with 0.5 μg plasmid/well on coverslips. The cells on the coverslips were fixed in 4% formaldehyde in PBS for 10 mins at room temperature. The fixed cells were then permeabilized and non-specific protein sites blocked with GTP buffer (2% goat serum, 0.2% Triton X-100, in PBS) for 30 mins at room temperature. Coverslips were then

incubated with mouse monoclonal anti-HA primary antibody, 1/15 dilution from 2.5 μg/μl stock, in GTP buffer for 1 hr at 37°C. Cells were then washed three times, 5 mins/wash, in GTP buffer. Bound primary antibody was detected by incubating the cells with secondary antibody; goat anti-mouse Texas Red conjugated, at a 1/30 dilution for 1 hr at 37°C. The cells were washed as described above, rinsed in water and mounted on frosted microscope slides with mounting media (1 mg/ml *p*-phenylenediamine in 100 mM Tris-HCl (pH 8.0), 90% glycerol). Coverslips were attached to the slides by coating the edges with clear nail polish. The stained cells were examined by fluorescence using an Olympus BHA microscope in the rhodamine channel.

2.2.18 Hoechst Dye Fluorescent Nuclear Stain

The procedure for nuclear staining utilizing Hoechst Dye, was provided by Millipore. Cells were plated at 2.0×10^5 on coverslips and grown to confluency at which time the cells were fixed and permeabilized by incubating at –70°C in ice cold methanol for 10 mins. At this time the cells were washed once with PBS and incubated with the Hoechst 33258 dye (0.25 mg/ml in purified water) at 37°C for 4 hrs. After incubation with the dye the coverslips were rinsed in water and mounted on frosted microscope slides with mounting media (1 mg/ml *p*-phenylenediamine in 100 mM Tris-HCl (pH 8.0), 90% glycerol). The coverslips were then attached to the slides by coating the edges with clear nail polish and viewed under an Olympus BHA microscope using the fluorescein channel.

CHAPTER THREE

RESULTS

3.1 Dihybrid Screen

In order to gain a better understanding of how transcriptional regulation occurs, and more specifically how PPARα activity is regulated, we sought to find PPARα interacting proteins that could also be PPARα modulators. The yeast dihybrid system provides one method of screening, *in vivo*, a large number of proteins for potential interacting partners. Consequently, an amino-terminal truncation of mPPARα (aa 83-486) was used to screen a Matchmaker human liver cDNA library. Kenji Miyata performed the dihybrid screen.

One of the potential colonies turned a light blue colour with a β-galactosidase assay. This potential positive colony contained the amino terminus of mtHMG-CoAS (aa 1-345; Figure 3). We therefore cloned the full length human mtHMG-CoAS for further study. The carboxyl terminus of human mtHMG-CoAS, beginning at residue 144, was obtained from Boukaftane *et al.*, 1994 and this was used in conjunction with the amino terminus from the dihybrid screen to construct the full length clone (Section 2.1.6.3).

3.2 *In Vitro* Solid Phase Capture and Immunoprecipitation Assay

To confirm the physical interaction between mPPARα and mtHMG-CoAS in yeast, an *in vitro* solid phase capture assay utilizing GST fusions was performed (Figure 4). GST fusions of both mPPARα and RXRα were constructed, expressed in bacteria and

A

1 **MQRLLTPVKRILQLTRAVQETSLTPARLLPVAHQRFS** TASAVPLAKTDTWPKDVGILALE

61 VYFPAQYVDQTDLEKYNNVEAGKYTVGLGQTRMGFCSVQEDINSLCLTVVQRLMERIQLP

121 WDSVGRLEVGTETIIDKSKAVKTVLMELFQDSGNTDIEGIDTTNACYGGTASLFNAANWM

181 ESSSWDGRYAMVVCGDIAVYPSGNARPTGGAGAVAMLIGPKAPLALERGLRGTHMENVYD

241 FYKPNLASEYPIVDGKLSIQCYLRALDRCYTSYRKKIQNQWKQAGSDRPFTLDDLQYMIF

301 HTPFCKMVQKSLARLMFNDFLSASSDTQTSLYKGLEAFGGLKLEDTYTNKDLDKALLKAS

361 QDMFDKKTKASLYLSTHNGNMYTSSLYGC ***LASLL***SHHSAQELAGSRIGAFSYGSGLAASF

421 FSFRVSQDAAPGSPLDKLVSSTSDLPKRLASRKCVSPEEFTEIMNQREQFYHKVNFSPPG

481 DTNSLFPGTWYLERVDEQHRRKYARRPV

B

1 MPGSLPLNAEACWPKDVGIVALEITFPSQYVDQAELEKYDGVDAGKYTIGLGQARMGFCT

61 DREDINSLCLTVVQNLMERNSLSYDCIGRLEVGTETIIDKSKSVKSNLMQLFEESGNTDI

121 EGIDTTNACYGGTAAVFNAVNWIESSSWDGRYALVVAGDIAIYATGNARPTGGVGAVALL

181 IGPNAPLIFDRGLRGTHMQHAYDFYKPDMLSEYPIVDGKLSIQCYLSALDRCYSVYRKKI

241 RAQWQKEGNDNDFTLNDFGFMISHSPYCKLVQKSLARMFLNDFLNDQNRDKNSIYSGLEA

301 FGDVKLEDTYFDRDVEKAFMKASSELFNQKTKASLLVSNQNGNMYTSSVYGS***LASVL***AQY

361 SPQQLAGKRIGVFSYGSGLAATLYSLKVTQDATPGSALDKVTASLCDLKSRLDSRTCVAP

421 DVFAENMKLREDTHHLANYIPQCSIDSLFEGTWYLVRVDEKHRRTYARRPSTNDHNLGDG

481 VGLVHSNTATEHIPSPAKKVPRLPATAAESESAVISNGEH

Figure 3: Amino acid sequence of mHMG-CoAS and cHMG-CoAS. (A) Sequence of full length human mHMG-CoAS. The sequence in bold signifies the putative mitochondrial targeting sequence, the sequence underlined represents the partial clone obtained through the yeast dihybrid screen and the sequence in italics and bold highlights the single LXXLL motif. The boxed sequence shows the clone obtained from Boukaftane *et al.*, 1994 that was used to construct the full length human mHMG-CoAS. (B) Sequence of full length hamster cHMG-CoAS, which was a generous gift from Gil *et al.*, 1995. The sequence in italics and bold highlights the corresponding LXXLL motif in the cytoplasmic enzyme which is LXXVL.

purified. Figure 4 illustrates the interaction of mtHMG-CoAS with both GST-mPPARα and GST-RXRα (lane 3) but not with GST (lane 6). The human cHMG-CoAS, which was going to be used as a control was unavailable. Hamster cHMG-CoAS, which possess 94.4% identity with the human enzyme, was readily available and since the two enzymes possess such a high identity, the hamster form was used as a control (Figure 3; Gil *et al.*, 1986, Mascaró *et al.*, 1994). cHMG-CoAS appeared to be unable to bind to either receptor (lane 4).

Quantification of the amount of mtHMG-CoAS that was retained by the GST fusion proteins was performed with the use of a Molecular Dynamics Phosphoimager. Approximately 0.5% of mtHMG-CoAS (lane 3) bound to GST-mPPARα compared to 26% of RXRα that bound to GST-mPPARα (lane 2). Approximately 1.5% of mtHMG-CoAS (lane 3) bound to GST-RXRα compared to 43% of mPPARα that bound to GST-RXRα (lane 2).

Since the observed *in vitro* interaction between mtHMG-CoAS and mPPARα and RXRα was weak, we sought to strengthen the *in vitro* data by using another *in vitro* binding assay, co-immunoprecipitations. Figure 5 illustrates again a selective interaction between mtHMG-CoAS and mPPARα and RXRα (lanes 6 and 12 respectively). As seen in the solid phase capture assays, approximately 0.5% of mtHMG-CoAS (lane 6) was co-immunoprecipitated with mPPARα whereas no mtHMG-CoAS was detected with preimmune sera (lane 5). Also, approximately 2% of mtHMG-CoAS was co-

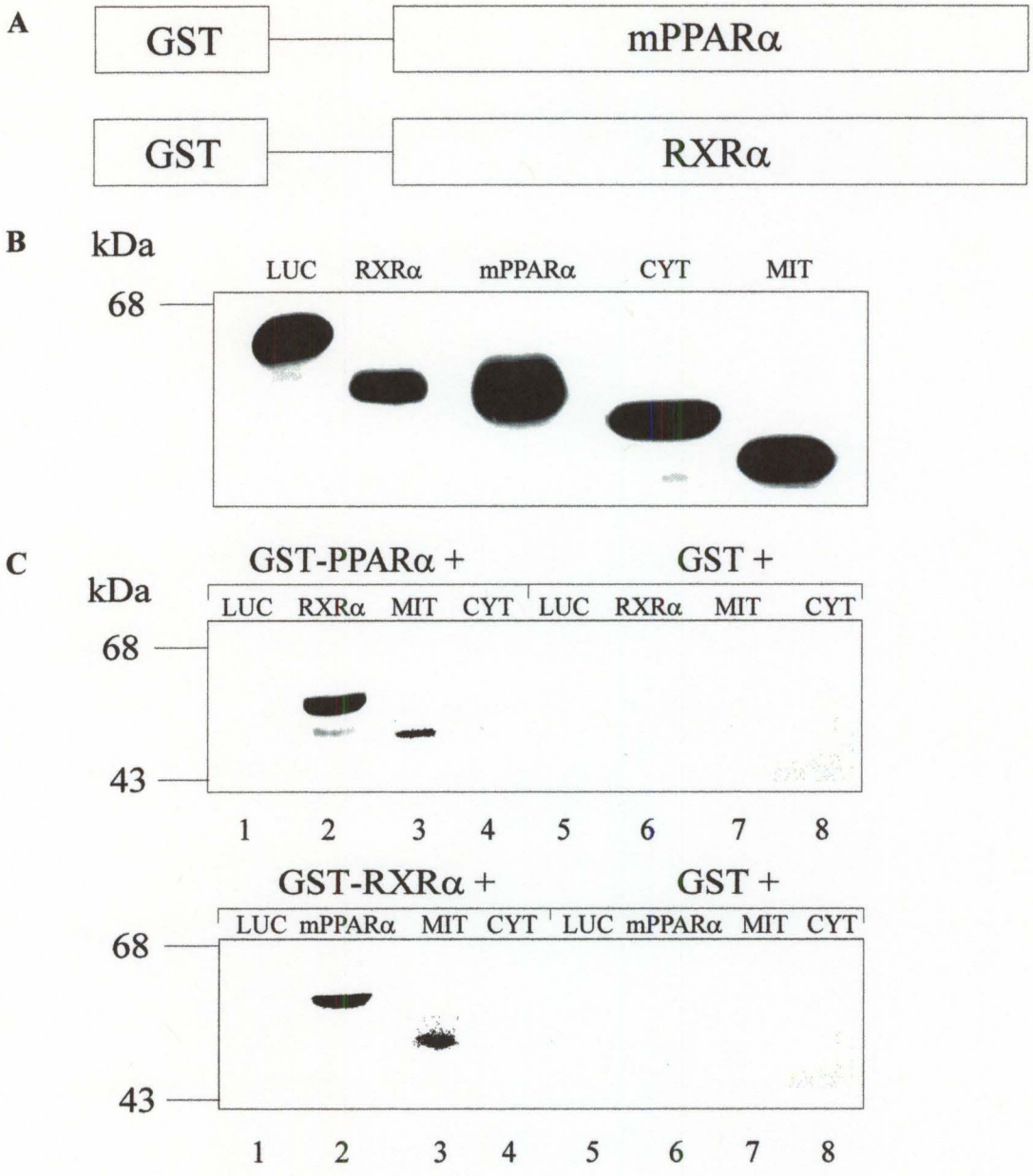

Figure 4: Solid phase capture assay that illustrates a specific interaction between mPPARα and RXRα and mHMG-CoAS. (A) Schematic representation of the two GST fusions used in the solid phase capture assays; GST-mPPARα and GST-RXRα. (B) Aliquots of *in vitro* L-[^{35}S]-methionine translated luciferase (LUC), RXRα, mPPARα, mHMG-CoAS (MIT) and cHMG-CoAS (CYT). (C) Aliquots of *in vitro* L-[^{35}S]-methionine translated luciferase (LUC), mPPARα, RXRα, mHMG-CoAS (MIT) and cHMG-CoAS (CYT) were incubated with either GST-mPPARα or GST-RXRα coupled beads. The beads were then washed and the bound proteins were eluted and resolved on a 10% polyacrylamide SDS-PAGE gel.

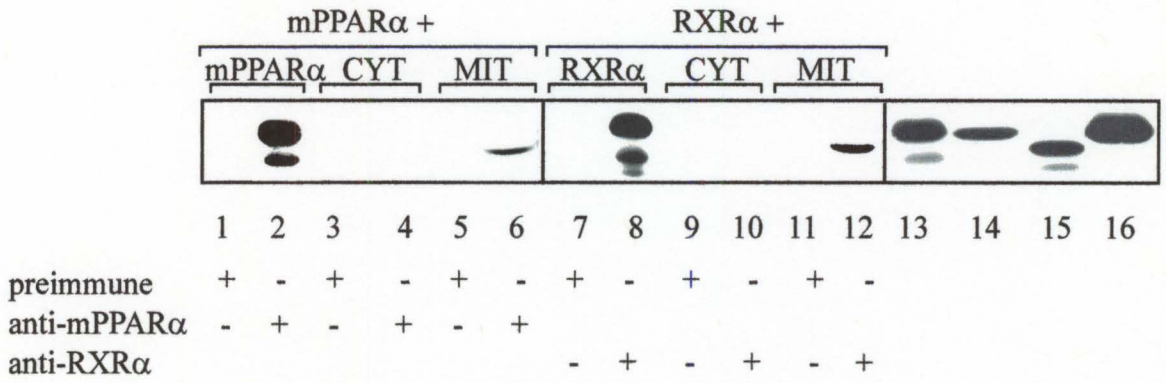

Figure 5: Immunoprecipitation assay that illustrates a specific interaction between mPPARα and RXRα and mHMG-CoAS. (A) Aliquots of *in vitro* L-[^{35}S]-methionine translated mPPARα, RXRα, cHMG-CoAS (CYT) and mHMG-CoAS (MIT) were incubated with either mPPARα or RXRα bound to their corresponding antibody coupled beads. The beads were then washed and the bound proteins were eluted and resolved on a 10% polyacrylamide SDS-PAGE gel. Lanes 13-16 are representatives of *in vitro* L-[^{35}S]-methionine translated mPPARα, cHMG-CoAS, mHMG-CoAS and RXRα.

immunoprecipitated with RXRα (lane12) while again no mtHMG-CoAS was detected with preimmune sera (lane 11). The percent of mtHMG-CoAS that was co-immunoprecipitated with either receptor is quite similar to that seen with the solid phase capture assays. Again, cHMG-CoAS showed no binding capabilities (lanes 4 and 10).

The solid phase capture/immunoprecipitation assays revealed that mtHMG-CoAS could interact with both mPPARα and RXRα *in vitro*. In addition, the interaction was specific to the mitochondrial enzyme. These assays did not determine which region(s) in either mtHMG-CoAS or mPPARα or RXRα was responsible for the observed interaction.

3.3 Effect of Ligand on Binding of mtHMG-CoAS to mPPARα and RXRα

Many nuclear receptor interacting proteins bind to their corresponding receptor in either a ligand-dependent or ligand-enhanced manner. To ascertain if the addition of either PPARα or RXRα ligand had any effect on the strength of the interaction with mtHMG-CoAS, *in vitro* solid phase capture assays utilizing GST fusions (Figure 4A) were performed (Figure 6). The ligand used for mPPARα was Wy-14-643 and for RXRα, 9-*cis* retinoic acid. As seen in Figure 6, the presence of vehicle (DMSO) or ligand had no effect on the ability of mtHMG-CoAS to interact with either mPPARα (lanes 2 and 3 respectively) or RXRα (lanes 5 and 6 respectively) when compared to the binding in the absence of vehicle or ligand (lanes 1 and 4).

3.4 Site-Directed Mutagenesis

During this time several papers were published that demonstrated the importance

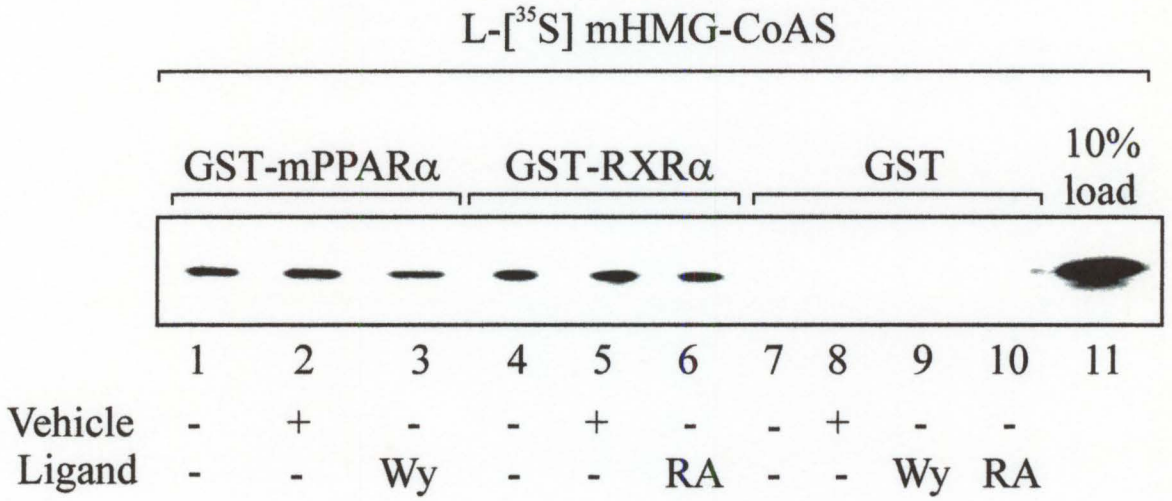

Figure 6: Solid phase capture assay that illustrates a specific ligand-independent interaction between mPPARα and RXRα and mHMG-CoAS. Aliquots of *in vitro* L-[^{35}S]-methionine translated mHMG-CoAS were incubated with either GST-mPPARα or GST-RXRα coupled beads alone or with 0.1 mM vehicle (DMSO), 0.1 mM Wy 14,643 (Wy) or 1 μM 9-*cis* retinoic acid (RA). The beads were then washed and the bound proteins were eluted and resolved on a 10% polyacrylamide SDS-PAGE gel.

of the motif, LXXLL, for the interaction between a nuclear receptor and a coactivator (Heery *et al.*, 1997, Zhu *et al.*, 1997). It was shown that the presence of the LXXLL motif in coactivators was at least partially responsible for their ability to interact with the ligand binding domain of a nuclear receptor.

Upon study of the mtHMG-CoAS peptide sequence, it was discovered that mtHMG-CoAS contains a single LXXLL motif. Consequently, to determine if the motif is responsible, at least partially, for the interaction detected between mtHMG-CoAS and mPPARα and RXRα, a site-directed mutant of the mtHMG-CoAS motif was constructed. The LASLL sequence in mtHMG-CoAS was changed to LASVL, a change in aa position 393 from a leucine to a valine (mtHMG-CoAS (L393V); Figure 7A). The cytoplasmic control enzyme does not contain a LXXLL motif. Its corresponding sequence is LASVL (Figure 7A).

3.5 *In Vitro* Immunoprecipitation with mtHMG-CoAS (L393V)

To determine if the LASLL motif in mtHMG-CoAS had a role in the observed interaction with mPPARα and RXRα, *in vitro* immunoprecipitations with the mutant were performed. As seen in Figure 7B, the mutant, mtHMG-CoAS (L393V), showed a substantial reduction, around five-fold, in its ability to interact with mPPARα (lane 4) and a two-fold reduction in its ability to bind RXRα (lane 10). The immunoprecipitation with the mutant interestingly revealed that the LASLL sequence in the mtHMG-CoAS protein was at least partially responsible for the proteins ability to interact with both mPPARα and

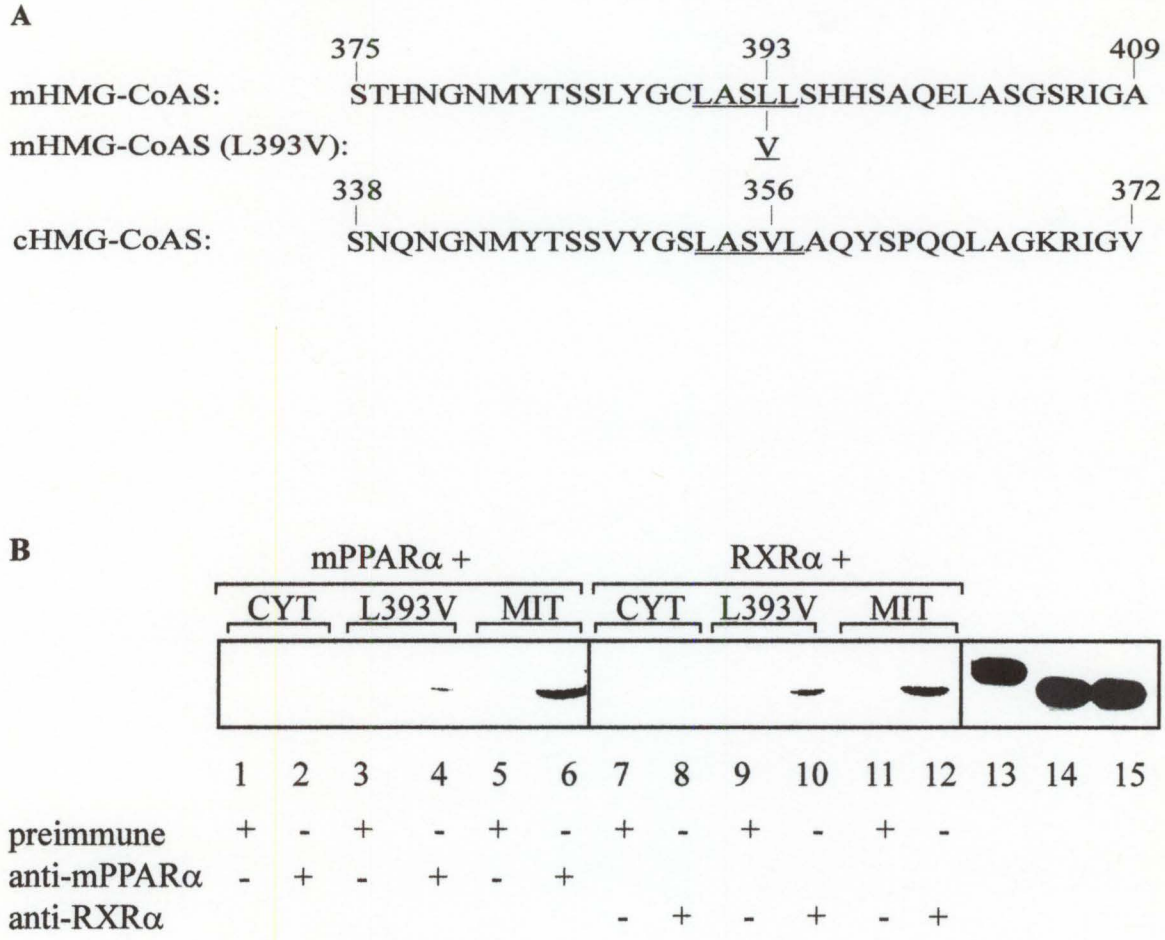

Figure 7: Immunoprecipitation assay that illustrates a reduced interaction between mHMG-CoAS (L393V) and mPPARα and RXRα. (A) Schematic representation of the LXXLL motif and its surrounding sequence in mHMG-CoAS, mHMG-CoAS (L393V) and cHMG-CoAS. (B)Aliquots of *in vitro* L-[^{35}S]-methionine translated cHMG-CoAS (CYT), mHMG-CoAS (L393V) and mHMG-CoAS (MIT) were incubated with mPPARα or RXRα bound to their corresponding antibody coupled beads. The beads were then washed and the bound proteins were eluted and resolved on a 10% polyacrylamide SDS-PAGE gel. Lanes 13-15 are representatives of *in vitro* L-[^{35}S]-methionine translated cHMG-CoAS, mHMG-CoAS (L393V) and mHMG-CoAS.

RXRα.

3.6 Electrophoretic Mobility Shift Assays (EMSAs)

Another important question that was addressed was what effect might mtHMG-CoAS have on the ability of mPPARα and RXRα to heterodimerize on a PPRE. That question was answered with the use of EMSAs. The HMG PPRE was chosen as one that would be important for study. Figure 8A shows that both mtHMG-CoAS and cHMG-CoAS led to approximately a 2 fold increase in complex formation followed by a decrease, as determined by phosphoimaging, and formation of a second lower band on the HMG PPRE. The exact nature of the second lower band has not been determined. To determine if mtHMG-CoAS or cHMG-CoAS would have a similar effect on mPPARα/RXRα heterodimerization on another PPRE, the AOx PPRE was used. On the AOx PPRE, Figure 8B, both mtHMG-CoAS and cHMG-CoAS showed a 50% decrease in mPPARα/RXRα complex formation as determined by phosphoimaging. These findings suggest that the effect of mtHMG-CoAS or cHMG-CoAS on the ability of mPPARα/RXRα to heterodimerize on DNA is PPRE specific. Exactly why both mtHMG-CoAS and cHMG-CoAS had the same effect on each PPRE is not entirely known. One possibility is examined in the discussion.

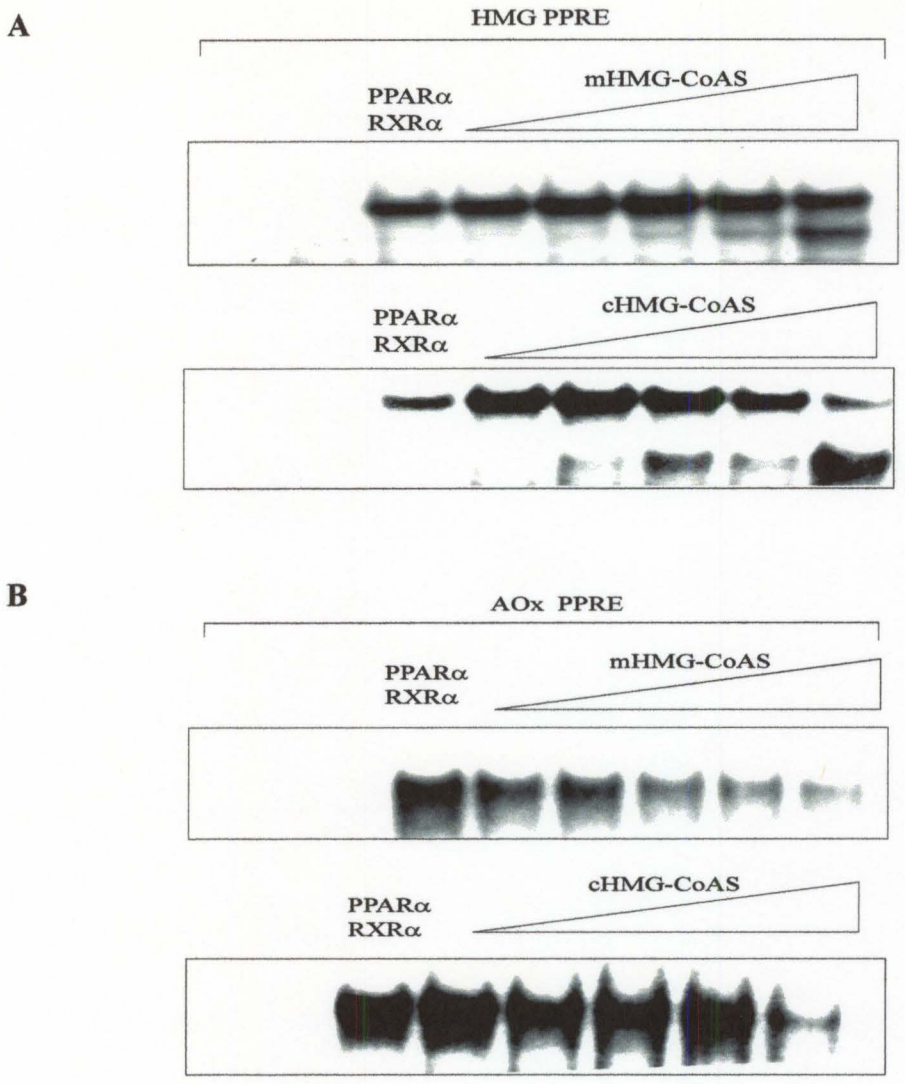

Figure 8: EMSAs to study the effect of mHMG-CoAS and cHMG-CoAS on mPPARα and RXRα binding on the HMG and AOx PPRE. (A) Titration of either mHMG-CoAS or cHMG-CoAS (0.5, 1, 2, 3 and 4 μl) against a constant amount of both mPPARα and RXRα (2 μl) on the HMG PPRE. *In vitro* non-radioactive proteins were incubated with [α–^{32}P]dATP labeled DNA. After incubation, the samples were run on a 4% non-denaturing acrylamide gel. (B) Titration of either mHMG-CoAS or cHMG-CoAS against constant amounts of mPPARα and RXRα on the AOx PPRE. The procedure used was the same as in (A).

3.7 Transient Transfection Assays

3.7.1 Introduction to the Elements used in the Transfections, the HMG and AOx PPRE

To ascertain if mtHMG-CoAS can modulate mPPARα activity within a cell, transient transfection assays were done in BSC40 cells. Reporter plasmids that contained the luciferase gene, the CPS promoter and various upstream PPREs were used. In addition, the PPARα ligand Wy-14,643 was used to study mPPARα mediated transactivation (Figure 9).

Addition of mPPARα and RXRα together on the 1 copy HMG PPRE led to repression of the activation that was seen by the receptors alone (Figure 9A). The repression was also down to basal levels. However, mPPARα showed a 2.5 fold drug response on the 1 copy HMG PPRE while ligand appeared to have no effect with RXRα. The presence of mPPARα transactivation and the absence of mPPARα/RXRα transactivation has previously been detected (Rodríguez *et al.,* 1994). However, the exact reasons behind the absence of mPPARα/RXRα transactivation have not been elucidated. It was initially thought that perhaps the HMG PPRE might require 2 copies of its cognate sequence before mPPARα/RXRα transactivation could be detected.

Consequently, a tandem 2 copy HMG PPRE was constructed and used in transient transfections. It too led to repression of transactivation upon the addition of both receptors (Figure 9A). Also, like the 1 copy HMG PPRE, the 2 copy HMG PPRE

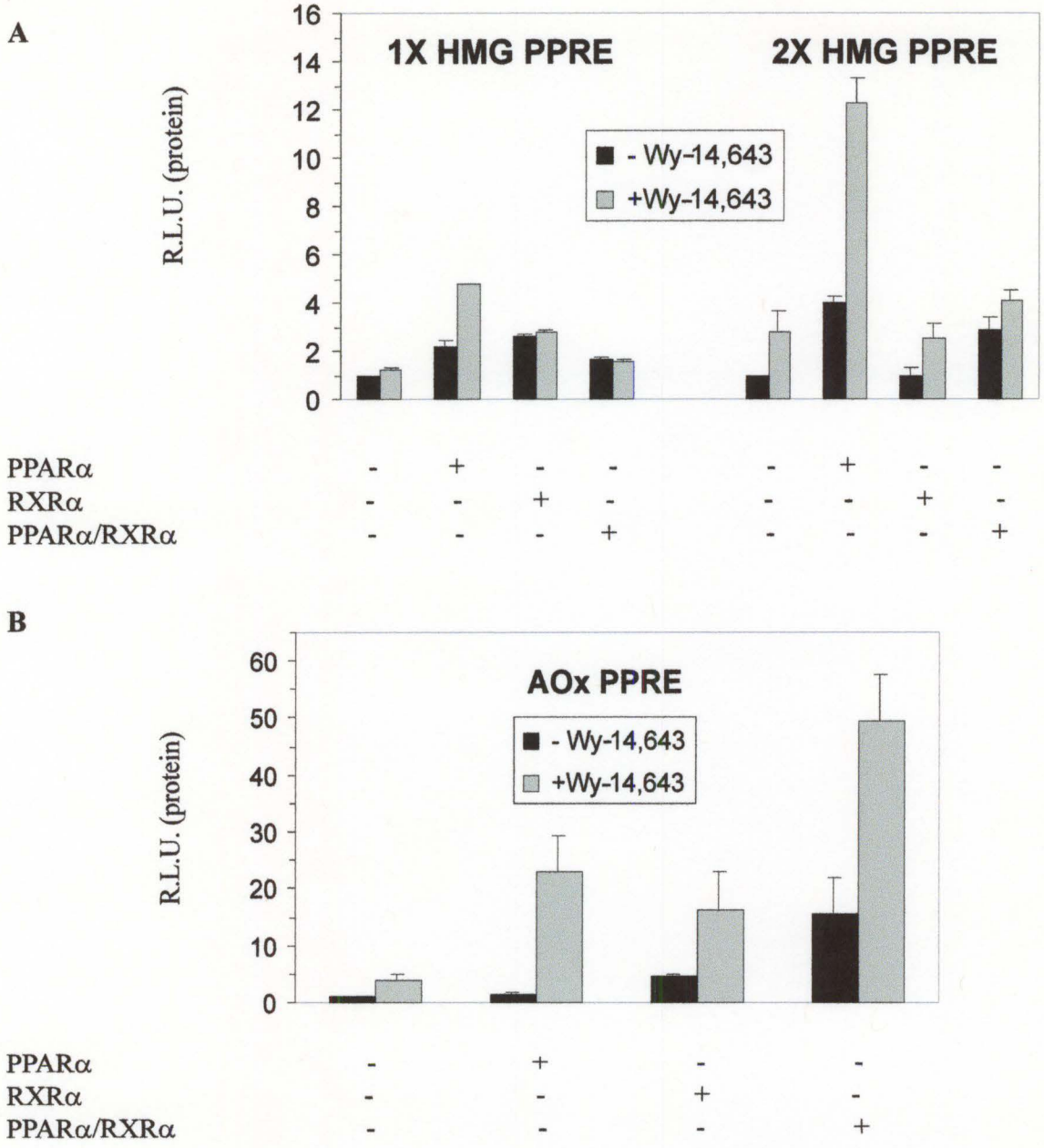

Figure 9: Transient transfection assay illustrating a PPRE dependent response with the addition of mPPARα and RXRα. (A) and (B) BSC40 cells were transfected by the calcium phosphate method with 1.25 μg pCPS-Luc-1 or 2X HMG PPRE or the 2X AOx PPRE, 0.5 μg mPPARα, RXRα or both. Each transfection mix was divided equally over four wells, 2 which were duplicates containing 0.1 mM Wy-14,643 with the other two containing 0.1 mM vehicle (DMSO). The cells were harvested 24 hrs after the media change. The lysates were assayed for luciferase activity in relative light units (R.L.U.) and adjusted for protein content. The data presented here was based on two separate assays, each done in duplicate.

showed a strong drug dependent response with mPPARα. Also the 2 copy HMG PPRE showed better mPPARα transactivation than the 1 copy, around 13 fold over reporter alone compared to 5 fold respectively.

Therefore, it appears that mPPARα mediated transactivation on the HMG PPRE is inhibited upon addition of exogenous RXRα. The exact reasons behind this observation have not been fully determined. One possible scenario is described in the discussion. It should also be noted that the 1 copy HMG PPRE was used in all future transient transfection experiments using the HMG PPRE.

A 2 copy AOx PPRE was chosen as a control as in the EMSAs. It has previously been shown that the AOx PPRE requires 2 copies of its motif before mPPARα/RXRα transactivation can be achieved. The AOx PPRE yielded the typical PPRE response, that is, activation of the reporter plasmid, around 50 fold over reporter alone, upon the addition of mPPARα and RXRα (Figure 9B).

3.7.2 Effect of mtHMG-CoAS, mtHMG-CoAS (L393V) and cHMG-CoAS on mPPARα/RXRα Mediated Transactivation on the HMG PPRE

Transient transfections were now performed to determine what effect mtHMG-CoAS might have in modulating mPPARα/RXRα transactivation of the HMG PPRE. Figure 10 illustrates the ability of mtHMG-CoAS, mtHMG-CoAS (L393V) and cHMG-CoAS to modulate mPPARα/RXRα activity on the HMG PPRE. It appeared that mtHMG-CoAS was able to potentiate transcriptional activation via its own PPRE, around

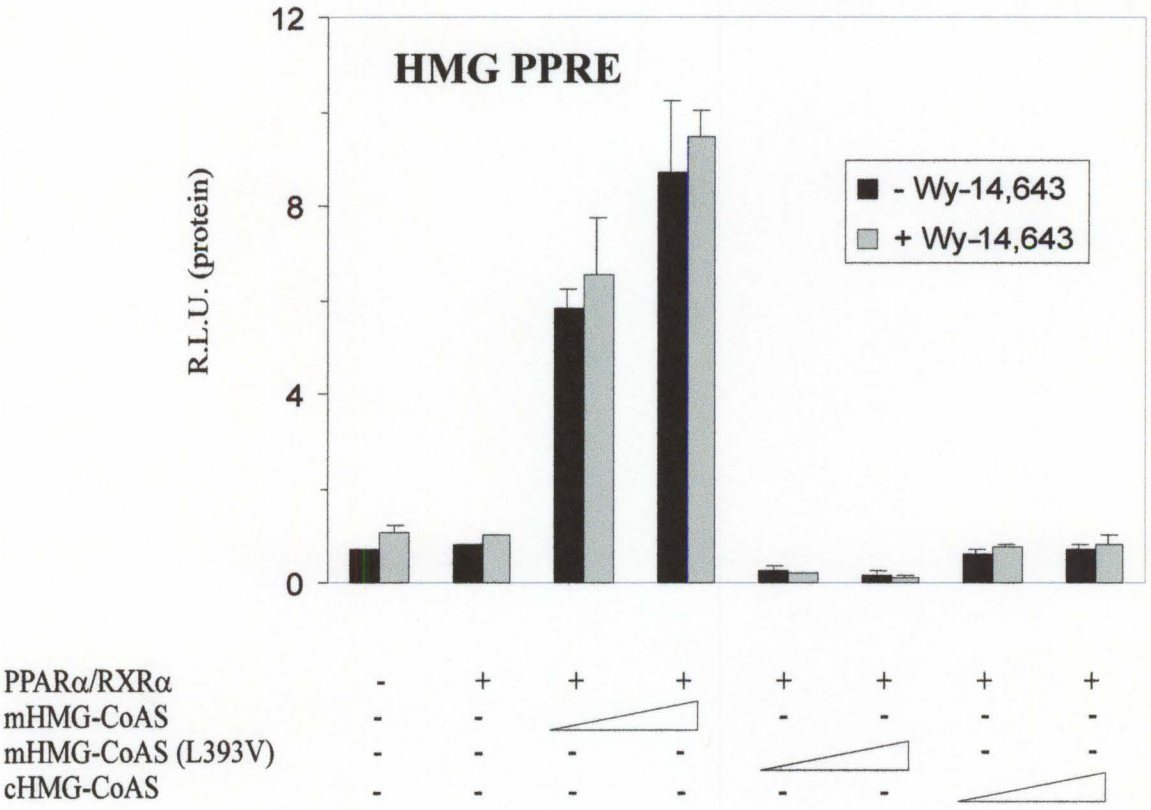

Figure 10: Transient transfection assay illustrating the effect of mHMG-CoAS, mHMG-CoAS (L393V) and cHMG-CoAS on mPPARα/RXRα mediated transactivation on the HMG PPRE. BSC40 cells were transfected by the calcium phosphate method with 1.25 μg pCPS-Luc-1X HMG PPRE, 0.5 μg mPPARα/RXRα, and 1.25/2.5 μg of either mHMG-CoAS, mHMG-CoAS (L393V) or cHMG-CoAS. Each transfection mix was divided equally over four wells, 2 which were duplicates containing 0.1 mM Wy-14,643 with the other two containing 0.1 mM vehicle (DMSO). The cells were harvested 24 hrs after the media change. The lysates were assayed for luciferase activity in relative light units (R.L.U.) and adjusted for protein content. The data presented here was based on two separate assays, each done in duplicate.

10 fold over reporter alone at the highest concentration used. The mutant, mtHMG-CoAS (L393V) seemed to inhibit mPPARα/RXRα mediated transactivation to below basal levels at all concentrations. The cytoplasmic control enzyme had no effect on mPPARα/RXRα transactivation.

3.7.3 Effect of mtHMG-CoAS, mtHMG-CoAS (L393V) and cHMG-CoAS on mPPARα Mediated Transactivation on the HMG PPRE

Since mPPARα alone showed better transactivation capabilities on the HMG PPRE than in the presence of RXRα, the effect of mtHMG-CoAS on mPPARα mediated transactivation was determined. The following experiment is identical to the one described above except that in this case RXRα was not used (Figure 11A and B). As when both mPPARα and RXRα were present, mtHMG-CoAS potentiated mPPARα mediated transactivation. Also, the mtHMG-CoAS potentiated mPPARα transactivation to a much greater extent when PPARα was present alone, around 300 fold over reporter alone at the highest concentration used. Again, the mutant reduced transactivation to around basal levels at the highest concentration used. The cHMG-CoAS control enzyme had no significant effect.

3.7.4 Effect of mtHMG-CoAS, mtHMG-CoAS (L393V) and cHMG-CoAS on mPPARα/RXRα Mediated Transactivation on the AOx PPRE

To ascertain if mtHMG-CoAS is able to potentate mPPARα mediated transactivation on another PPRE, the AOx PPRE was used in conjunction with both

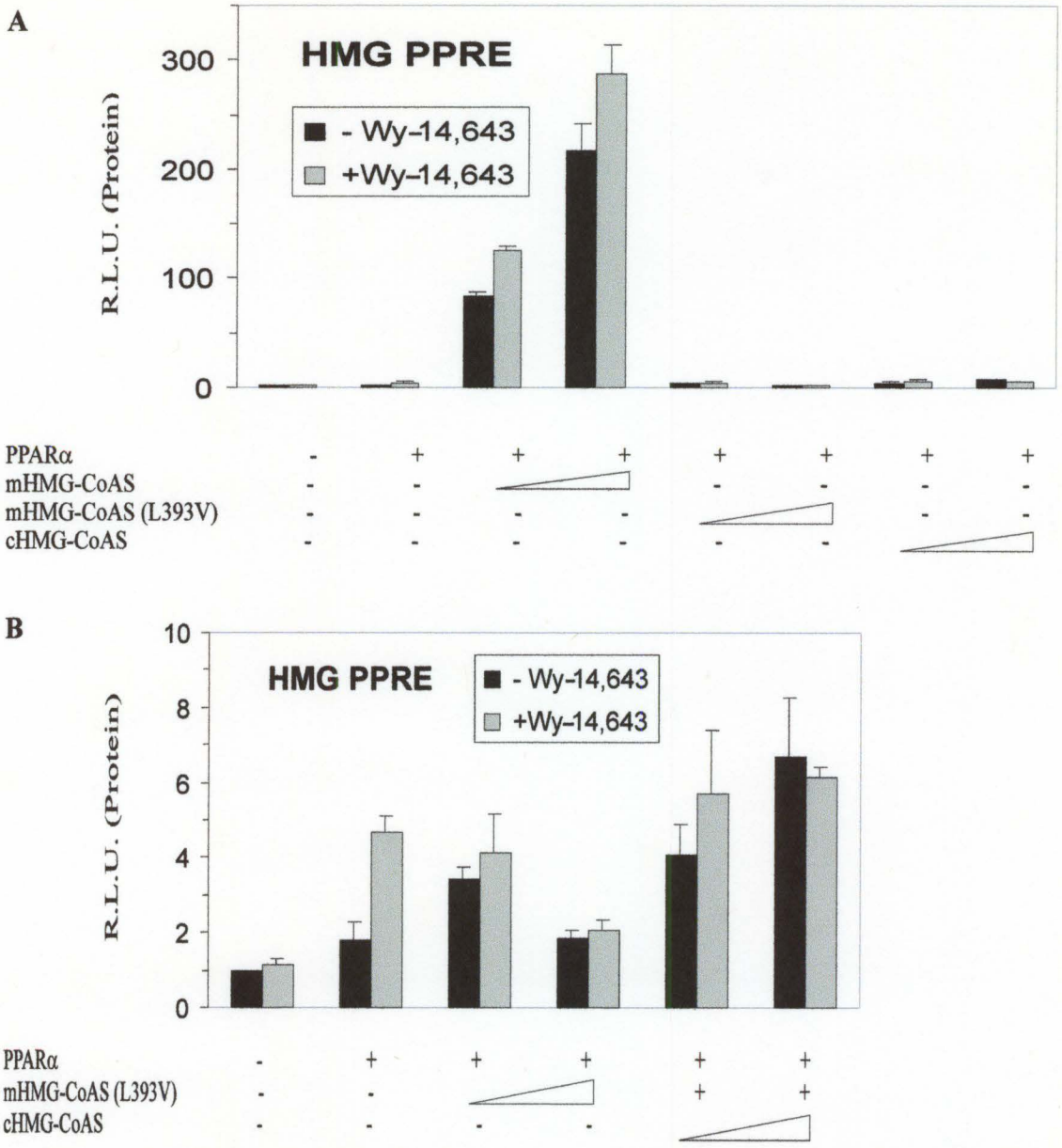

Figure 11: Transient transfection assay illustrating the effect of mHMG-CoAS, mHMG-CoAS (L393V) and cHMG-CoAS on mPPARα mediated transactivation on the HMG PPRE. (A) BSC40 cells were transfected by the calcium phosphate method with 1.25 μg pCPS-Luc-1X HMG PPRE, 0.5 μg mPPARα/RXRα, and 1.25/2.5 μg of either mHMG-CoAS, mHMG-CoAS (L393V) or cHMG-CoAS. Each transfection mix was divided equally over four wells, 2 which were duplicates containing 0.1 mM Wy-14,643 with the other two containing 0.1 mM vehicle (DMSO). The cells were harvested 24 hrs after the media change. The lysates were assayed for luciferase activity in relative light units (R.L.U.) and adjusted for protein content. The data presented here was based on two separate assays, each done in duplicate. (B) Same graph as (A) without the data for mHMG-CoAS.

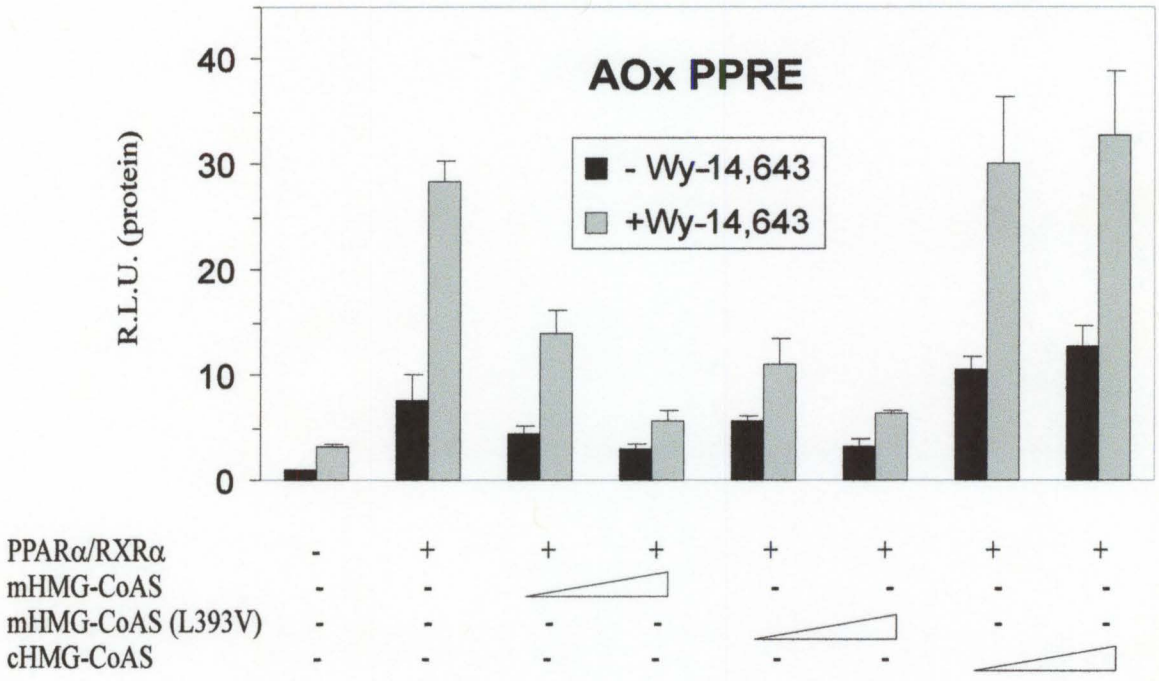

Figure 12: Transient transfection assay illustrating the effect of mHMG-CoAS, mHMG-CoAS (L393V) and cHMG-CoAS on mPPARα/RXRα mediated transactivation on the AOx PPRE. BSC40 cells were transfected by the calcium phosphate method with 1.25 μg pCPS-Luc-2X AOx PPRE, 0.5 μg mPPARα/RXRα, and 1.25/2.5 μg of either mHMG-CoAS, mHMG-CoAS (L393V) or cHMG-CoAS. Each transfection mix was divided equally over four wells, 2 which were duplicates containing 0.1 mM Wy-14,643 with the other two containing 0.1 mM vehicle (DMSO). The cells were harvested 24 hrs after the media change. The lysates were assayed for luciferase activity in relative light units (R.L.U.) and adjusted for protein content. The data presented here was based on two separate assays, each done in duplicate.

mPPARα and RXRα (Figure 12). On this PPRE, mtHMG-CoAS reduced the transactivation of mPPARα/RXRα by around 6 fold at the highest concentration used. Consequently, in transient transfection assays, as with the EMSAs, mtHMG-CoAS behaved in a PPRE dependent manner. The mutant, on the other hand, showed a similar effect on the AOx PPRE, it reduced mPPARα/RXRα transactivation by 6 fold at the highest concentration used. Therefore, it appears that the mitochondrial mutant is behaving in a dominant-negative fashion irrespective of the PPRE. Possible mechanisms to describe the PPRE dependent and dominant-negative effect of mtHMG-CoAS and the mutant respectively are outlined in the discussion. Again, cHMG-CoAS had no apparent effect.

3.8 Cellular Localization of mtHMG-CoAS, mtHMG-CoAS (L393V) and cHMG-CoAS

3.8.1 Background Information

Since mtHMG-CoAS appeared to be modulating mPPARα mediated transactivation, which occurs in the nucleus, one would intuitively suspect that some mtHMG-CoAS would be present in the nucleus. Consequently, the cellular localization of mtHMG-CoAS was determined. Since no antibodies for mtHMG-CoAS were readily available, hemagglutinin (HA) epitope tagged fusions of mtHMG-CoAS, mtHMG-CoAS (L393V) and cHMG-CoAS were constructed (Figure 13A).

3.8.2 Effect of the Hemagglutinin (HA) Tag on mtHMG-CoAS

To ensure that the HA tag was not affecting the selective ability of mtHMG-CoAS to bind to both mPPARα and RXRα, a solid phase capture assay utilizing GST fusions (Figure 5A) was performed (Figure 13B). As seen in lanes 3 and 5, mtHMG-CoAS-HA was still able to selectively bind to both mPPARα and RXRα and not GST alone (lane 1) while HA-cHMG-CoAS (lanes 4 and 6) did not interact with either receptor. Also, the HA tag did not reduce or enhance the ability of mtHMG-CoAS to bind to either receptor. mtHMG-CoAS-HA bound with about 1% efficiency to either receptor which was quite similar to that seen with the untagged version in both solid phase capture and immunoprecipitation assays. Lastly, to ensure that the HA tag was not interfering with the ability of mtHMG-CoAS to potentate mPPARα mediated transactivation, transient transfections were done on the HMG PPRE (Figure 13C). As seen in Figure 13C, mtHMG-CoAS-HA was still able to lead to mPPARα mediated transactivation, 50 fold over reporter alone at the highest concentration used. Both mtHMG-CoAS (L393V)-HA and HA-cHMG-CoAS did not potentate transactivation which is consistent with that seen with the untagged versions.

3.8.3 Immunofluorescence of mtHMG-CoAS-HA, mtHMG-CoAS (L393V)-HA and HA-cHMG-CoAS

When it was determined that the HA tag did not interfere with either mtHMG-CoAS ability to bind to both mPPARα and RXRα or its ability to lead to mPPARα

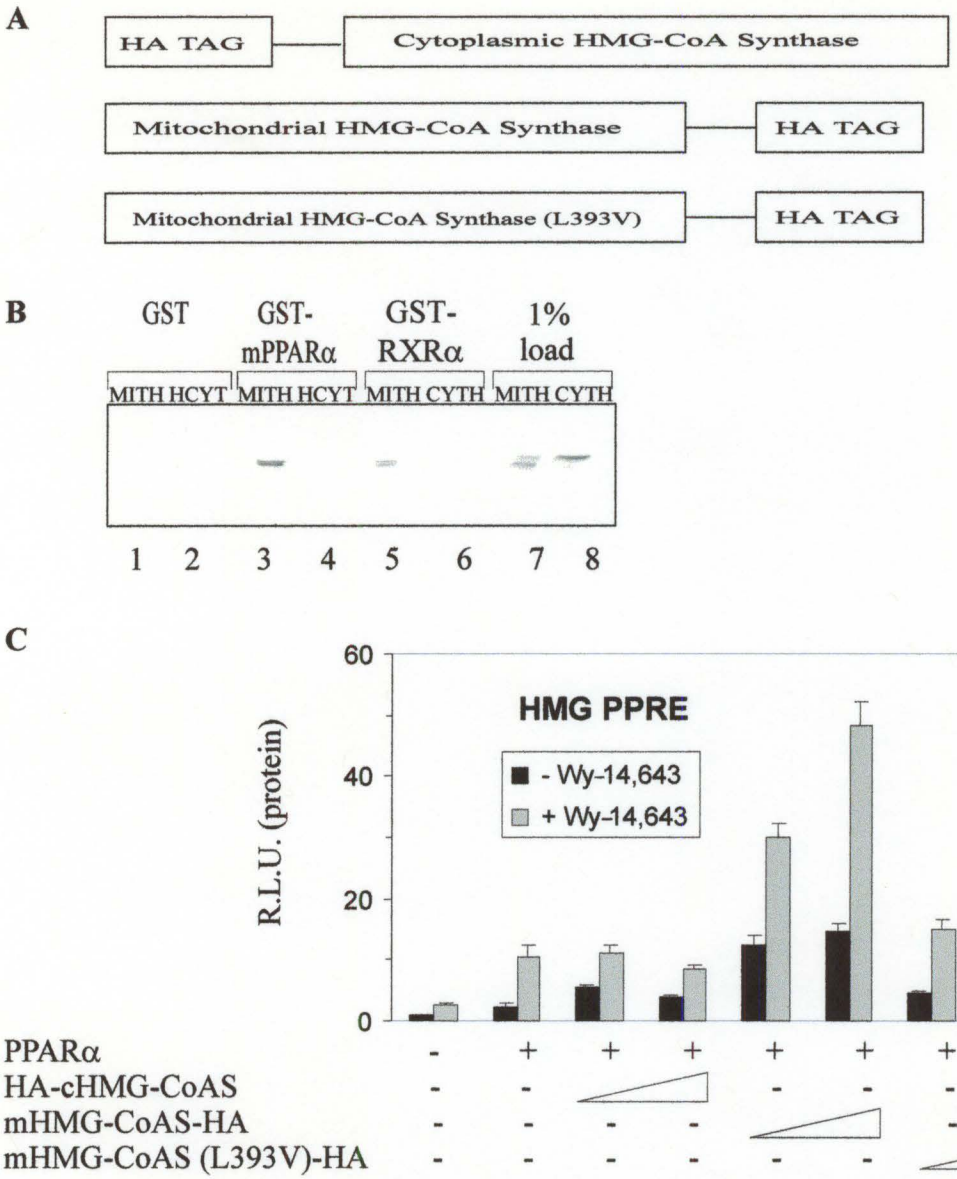

Figure 13: Effect of the presence of a hemagglutinin (HA) tag on the ability of mHMG-CoAS to bind to mPPARα or RXRα and lead to mPPARα mediated transactivation. (A) Schematic representation of the hemagglutinin (HA) epitope tag plasmids that were constructed for immunofluoresence studies. (B) Aliquots of *in vitro* L-[^{35}S]-methionine translated mHMG-CoAS-HA (MITH) and HA-cHMG-CoAS (HCYT) were incubated with either GST-mPPARα or GST-RXRα coupled beads. The rest of the procedure is the same as in Figure 4. (C) BSC40 cells were transfected by the calcium phosphate method with 1.25 μg pCPS-LUC-1X HMG PPRE, 0.5 μg of mPPAR, and 1.25/2.5 μg of either HA-cHMG-CoAS, mHMG-CoAS-HA or mHMG-CoAS (L393V)-HA. The rest of the procedure is the same as in Figures 9-12.

mediated transactivation, immunofluorescence was performed with the HA constructs in Cos-1 cells (Figure 14). Figure 14A contains the pictures of the transiently expressed HA plasmids (panels III to VII). As seen in Figure 14A, the HA constructs showed immunofluorescence above background (untransfected cells; panel I). Panels III and V show localization of both mtHMG-CoAS and the mutant to what appears to be the mitochondria. This is consistent with previous studies done on the cellular localization of the rat mtHMG-CoAS (Royo *et al.*, 1995).

There exists many methods by which proteins are localized to different compartments within the cell (Danpure, 1995). One such example is rat deoxyuridine triphosphatase (dUTPase) that requires the presence of PPARα for translocation from the cytoplasm to the nucleus. To determine if mPPARα has any effect on the localization of mtHMG-CoAS, mPPARα was co-transfected with the enzyme. When mPPARα was co-transfected with mtHMG-CoAS, in approximately 65% of the cells, localization of mtHMG-CoAS occurred at what appeared to be the mitochondria and the nucleus (panel IV). In contrast, when the mutant was co-transfected with mPPARα, localization remained solely in the mitochondria (panel VI).

The HA tagged control cHMG-CoAS was non-nuclear (panel VII). Panel II shows nuclear staining that was performed on Cos-1 cells using Hoechst dye. The nuclei seen in panel II are similar in size and shape to what is believed to be the nucleus in panel IV. The above results are summarized in Table 3.

Interestingly, it appears that mtHMG-CoAS requires the presence of mPPARα for nuclear localization. In addition, the nuclear localization is dependent on the integrity of the LASLL motif present in mtHMG-CoAS since the mutant remained non-nuclear. Therefore, it appears that mtHMG-CoAS relies on an interaction with mPPARα, through its LXXLL motif, for nuclear localization.

To ensure that all of the HA tagged constructs were being expressed, a Western blot was performed on Cos-1 cells that had been transiently transfected with the various HA tagged plasmids. As seen in Figure 14B, the HA tagged mtHMG-CoAS (lane 3), mutant (lane 5) and cHMG-CoAS (lane 7) are all expressed. Lanes 1 (untransfected) and 2 (mPPARα) show a cross- reactive band (x). The band x appeared to be running slightly higher than what appeared to be the mature form (m; with the targeting sequence removed) of mtHMG-CoAS. The precursor form of mtHMG-CoAS (p; with the mitochondrial targeting sequence) ran around 9 kDa higher than m which correlates with a 37 aa targeting sequence. Lane 7 contains cHMG-CoAS with no apparent processing.

It is also interesting to note that the presence of mPPARα did not appear to affect the processing capabilities of mtHMG-CoAS. It was thought that perhaps mPPARα was redirecting the unprocessed form of mtHMG-CoAS to the nucleus. However, there was no difference between the levels of mtHMG-CoAS p or m with the addition of mPPARα (lanes 3 and 4). mPPARα also had no significant affect on the mutants amount of p or m (lanes 5 and 6). It should be noted that the cells were harvested at the single time point of

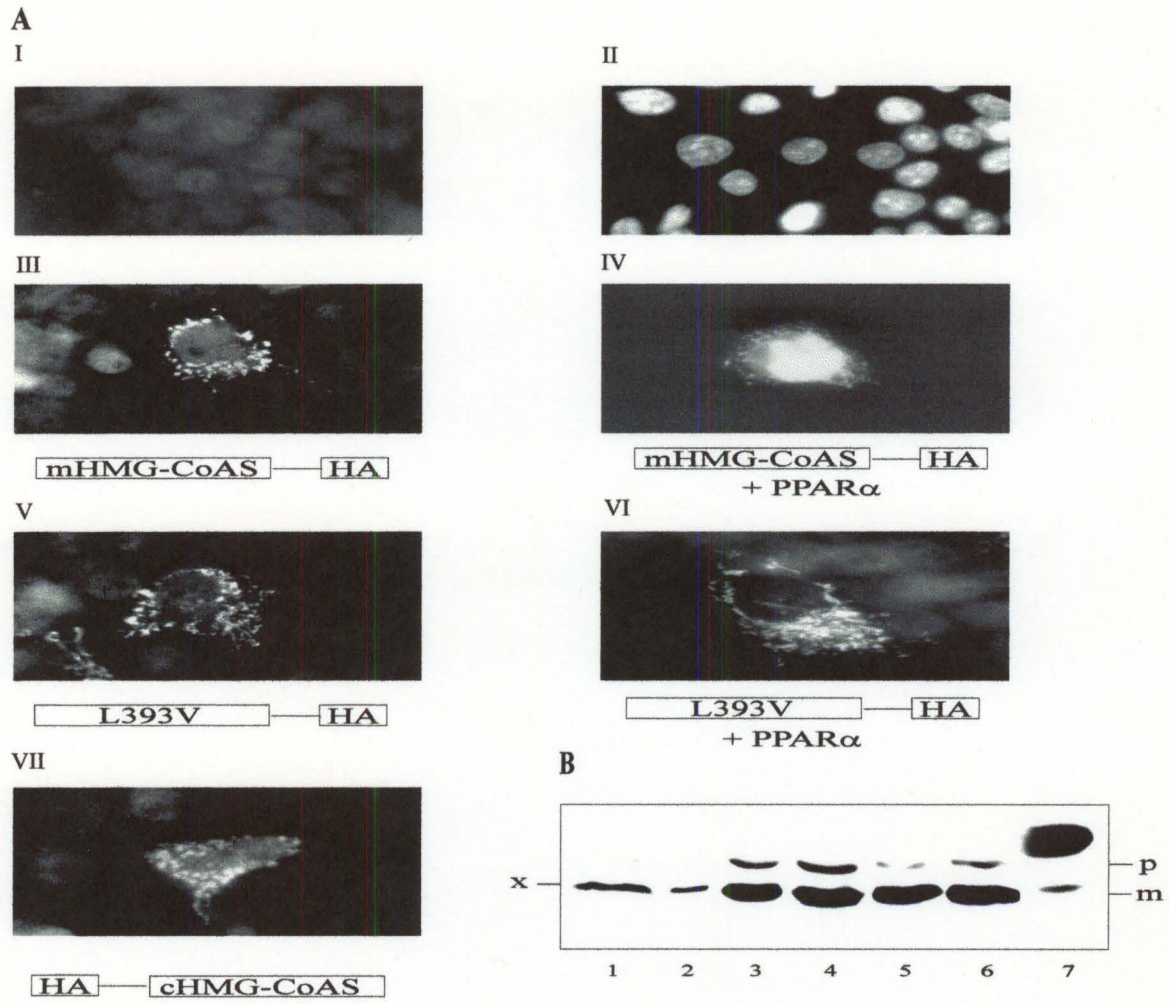

Figure 14: Immunofluoresence and Western blot of the various hemagglutinin (HA) epitope tagged constructs in Cos-1 cells: (A) Cos-1 cells were transfected on coverslips as in Figures 9-12, with 0.5 μg of each HA tagged plasmid/well in 0.1 mM DMSO. The cells were fixed and permeabilized. The 1°Ab was incubated with the cells. The cells were then washed. The 2°Ab was incubated with the cells and the cells were again washed. The coverslips were then mounted on microscope slides. Cells were visualized using immunofluorescence. (B) Cos-1 cells were transiently transfected, as in Figures 9-12, with 1.25 μg of each plasmid/well in 0.1 mM DMSO. Cells were harvested and run on a 10% SDS-PAGE gel, 100 μg total protein of each sample was loaded. The gel was transferred to nitrocellulose and the nitrocellulose was then blocked and washed. It was then incubated in 1^0 Ab and then washed again. The 2^0 Ab was then added and again the blot was incubated and washed as above. The nitrocellulose was then incubated with the detection solution and exposed to film. The symbols p, m and x represent precurosor form of mHMG-CoAS, mature form of mHMG-CoAS and cross-reactive band respectively. Panel I is background, panel II is nuclear staining, panel III is mHMG-CoAS-HA, panel IV is mHMG-CoAS co-transfected with PPARα, panel V is L393V-HA, panel VI is L393V-HA co-transfected with PPARα and panel VII is HA-cHMG-CoAS.

48 hrs post-transfection. In order to exclude the possibility of mPPARα affecting mtHMG-CoAS processing, several different time points should be studied.

3.8.4 Cellular Localization of HA-cHMG-CoAS and mtHMG-CoAS-HA in BSC40 cells

Since all of the transfection studies were done in BSC40 cells, to ensure that there were no differences in localization between Cos-1 and BSC40 cells, a few of the HA tagged constructs were chosen for immunofluorescence in BSC40 cells. As seen in Figure 15, HA-cHMG-CoAS was non-nuclear (panel II) and mtHMG-CoAS-HA was mitochondrial (panel III). Untransfected cells are seen in panel I. Consequently, the localization seen in Cos-1 cells is comparable to that seen in BSC40 cells.

Table 3: Summary of the Localization of the Various Hemagglutinin (HA) Epitope Tagged Constructs in Cos-1 cells

CLONE	LOCALIZATION		
	Mitochondria	Nucleus	Non-Nuclear
HA-cHMG-CoAS	-	-	+++
mtHMG-CoAS-HA	+++	-	-
mtHMG-CoAS-HA + PPARα	++	+++	
mtHMG-CoAS (L393V)-HA	+++	-	-
mtHMG-CoAS (L393V)-HA + PPARα	+++	-	-

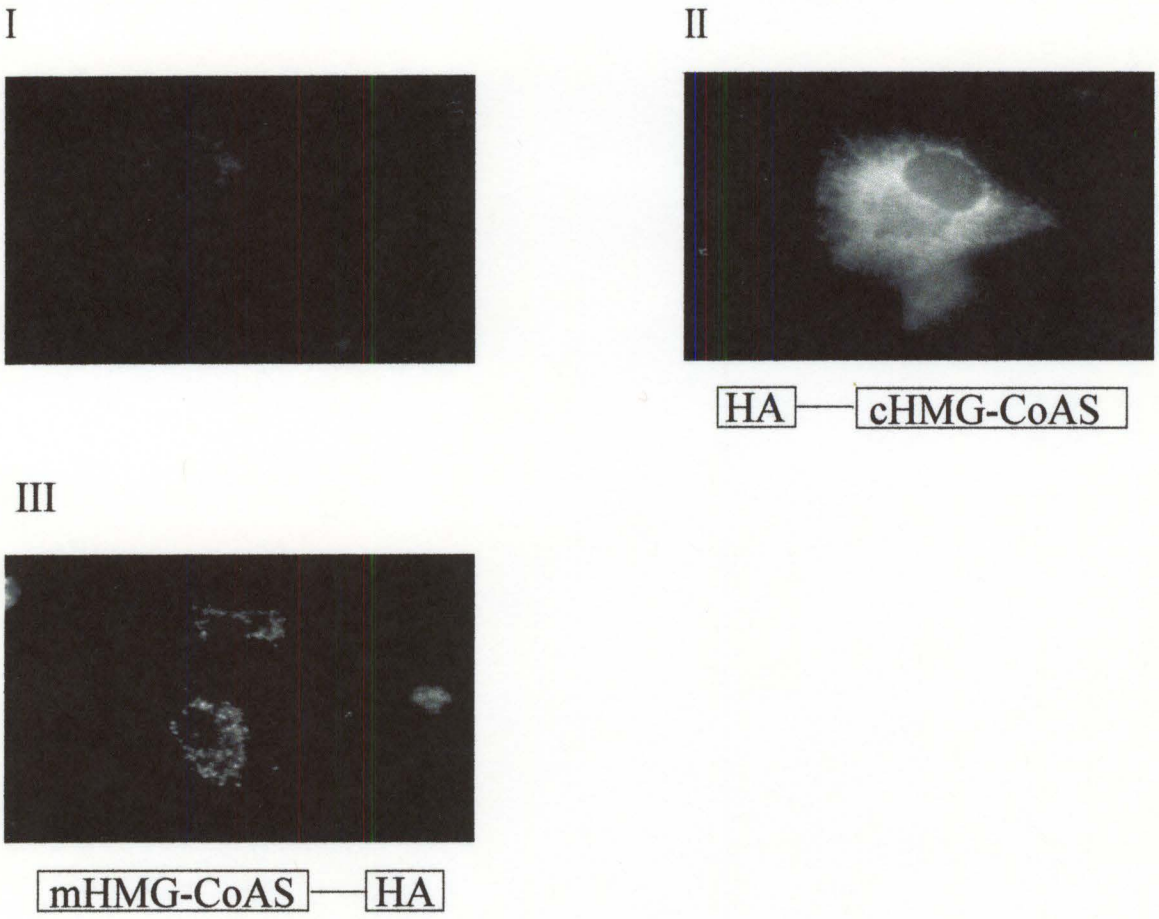

Figure 15: Immunofluorescence of a few hemagglutinin (HA) epitope tagged constructs in BSC40 cells: (A) BSC40 cells were transfected on coverslips, as described in Figures 9-12, with 0.5 μg of each HA tagged plasmid in 0.1 mM DMSO. The cells were fixed and permeabilized. The 1°Ab was incubated with the cells and the cells were then washed. The 2°Ab was incubated with the cells and then they were washed as above. The coverslips were then mounted on microscope slides and visualized using immunofluorescence. Panel 1 is background, panel II is HA-cHMG-CoAS and panel III is mHMG-CoAS-HA.

CHAPTER FOUR

DISCUSSION

4.1 *In Vitro* Binding Studies

Solid phase capture and immunoprecipitation assays confirmed the interaction between mtHMG-CoAS and mPPARα that was first detected in the dihybrid screen. The two *in vitro* assays also showed the interaction was specific to mtHMG-CoAS, cHMG-CoAS showed no binding capabilities, and that mtHMG-CoAS was also able to interact with RXRα. The identification of a specific interaction between nuclear hormone receptors and a mitochondrial enzyme is quite novel.

4.2 *In Vitro* Binding Studies with the L393V Mutant

Mutational analysis identified the LASLL motif in mtHMG-CoAS as being extremely important for the interaction between mtHMG-CoAS and nuclear hormone receptors. This is not the first time that a protein with a single LXXLL motif has been shown to be capable of both binding to receptors/coactivators and regulating their activity. An example of this is the coactivator P/CAF that contains a single LXXLL motif and interacts with RAR and CBP and modulates RAR mediated transactivation (Yang *et al.*, 1998). However, it is the first time that a LXXLL motif has been found to have a functional importance in a protein other than a coactivator.

The L393V mutation almost completely abolished the interaction with mPPARα and weakened the interaction with RXRα by 50%. Since L393V was still able to bind

albeit weakly to mPPARα, this would suggest that other determinants in mtHMG-CoAS might also contribute to binding. This is consistent with the fact that the partial mtHMG-CoAS cDNA clone isolated in the dihybrid screen lacked this region. Other coactivators, such as P/CAF, have been shown to possess interacting domains that are not completely dependent on the LXXLL motif (Korzus *et al.*, 1998). The reason why the mutation did not have a more drastic effect on RXRα is not clear. As with mPPARα, one can not eliminate the possibility of another interacting interface between RXRα and mtHMG-CoAS that is independent of the LXXLL motif.

Lastly, it is important to note the specificity of the regulation. It is only the mitochondrial synthase that contains the LXXLL motif, the corresponding human cytoplasmic form, even though it has 66% identity with the mitochondrial form, has the sequence LXXVL. This is not only the case in humans, but in all species currently known to contain both a single mitochondrial and cytoplasmic HMG-CoAS.

4.3 *In Vitro* Binding Studies with Ligand

The absence of a ligand-dependent interaction between mPPARα/RXRα and mtHMG-CoAS is also quite interesting. Generally, for proteins whose binding is mediated at least in part by a LXXLL motif, binding is highly dependent on the presence of ligand (reviewed in Shibata *et al.*, 1997). Recent evidence however, suggests that this is not always the case. For example, RIP140 contains 9 LXXLL motifs and binds to mPPARα in a manner that is not influenced by the presence of ligand (Miyata *et al.*, 1998). Futhermore, PPAR has been shown to interact in a ligand-independent manner with

coactivators including CBP (with PPARα) and SRC-1 (with PPARγ) (Zhu *et al.*, 1996, Dowell *et al.*, 1997). Consequently, it appears there are exceptions to the rule that coactivators can only bind to receptors in the presence of ligand.

4.4 Transient Transfections

The HMG and AOx PPRE behaved quite differently in response to exogenously added mPPARα and RXRα. The AOx PPRE illustrated the typical response, activation in the presence of both receptors while the HMG PPRE showed inhibition when compared to individually added mPPARα or RXRα. This might be the case if the AOx PPRE is not able to recruit endogenous RXRα as well as the HMG PPRE. If the HMG PPRE is able to recruit RXRα to a much better extent than the AOx PPRE, then when exogenous RXRα is added, squelching occurs.

The mitochondrial HMG-CoAS was not only capable of interacting with nuclear hormone receptors but was also able to modulate transcription by regulating a nuclear receptors activity. Enzymes have previously been shown to be capable of modulating transcription. One such example is rat dUTPase which has been shown to act as an inhibitor of PPARα. (Chu *et al.*, 1996). However, this is the first time that an enzyme has been shown to exert a PPRE dependent response. The fact that mtHMG-CoAS was able to activate on the HMG PPRE but inhibit on the AOx PPRE illustrates a specific pathway which allows for controlled and specific regulation of two different genes.

Keteogenesis is a very important mechanism for obtaining fuel for different organs of the body during extreme circumstances such as starvation, prolonged exercise or

diabetes. During such instances, mitochondrial HMG-CoAS is known to be a key regulatory enzyme. Therefore, perhaps the potentiation of mPPARα by mtHMG-CoAS allows for quick amplification of its own mRNA. This would lead to an increase in the amount of mtHMG-CoAS enzyme that would subsequently provide an increase in ketone bodies, or fuel, for the body.

The AOx enzyme is involved in β-oxidation within the peroxisome. The β-oxidation of fatty acids is increased during ketogenesis in order to provide acetyl-CoA, one of the initial substrates in the ketogenic pathway. Both the mitochondria and the peroxisome are involved in the β-oxidation of fatty acids and there has been much debate as to which system, if not both, is activated during ketogenesis. There has been some evidence suggesting that the rat liver AOx enzyme actually shows a decline in activity during starvation (Slauter and Yamazaki, 1984). This decline in activity of the AOx enzyme correlates with the inhibition seen on the AOx PPRE with the addition of mtHMG-CoAS in the transient transfection assays. The observed decline in the AOx catalytic activity during starvation was attributed to a reduction in total liver protein. However, perhaps mtHMG-CoAS is involved in down regulating peroxisomal β–oxidation and consequently, during extreme circumstances like starvation, the mitochondrial β-oxidation pathway becomes the main pathway for acetyl-CoA production.

Mitochondrial HMG-CoAS (L393V) inhibited transactivation on both the HMG and AOx PPRE. Previous work with SRC-1 has shown that when the LXXLL motifs were mutated in such a way that binding between SRC-1 and the estrogen receptors was

hindered, the mutated coactivator then inhibited transactivation, to below basal levels, in transient transfection assays (Heery *et al.*, 1997). It has been suggested that this is due to the coactivator being able to still interact with another factor important in either the assembly of the coactivator complex or the basal transcriptional machinery. Consequently, the dominant-negative effect seen with mtHMG-CoAS (L393V) might be due to its ability to bind to a limiting downstream effector target(s) of PPARα.

4.5 Localization Studies

The relevance of an interaction between a mitochondrial protein and a nuclear receptor is an important issue. However, proteins, including those previously believed to be found solely in mitochondria, have been found in more than one compartment (Soltys and Gupta, 1996, Handley-Gearhart *et al.*, 1994). Consequently, the question whether or not mtHMG-CoAS could be detected in another compartment, specifically the nucleus, was addressed.

When the HA tag was present at the carboxyl terminus of either human mtHMG-CoAS or the L393V mutant, the protein localized to the mitochondria. This is consistent with previous work that has shown mitochondrial localization for rat mtHMG-CoAS (Royo *et al.*, 1995). However, there are various mechanisms that have been proposed for the targeting of proteins to different cellular compartments. These include alternative transcription initiation, alternative translation initiation, alternative RNA splicing, competition between targeting sequences, post-translational modification and trans-acting factors (Danpure, 1995). A specific example of a protein being re-located is the rat dUTPase that appears to be a mediator of PPARα and requires the presence of PPARα

for translocation from the cytoplasm to the nucleus (Chu *et al.*, 1996).

Strikingly, when mPPARα was co-transfected with mtHMG-CoAS-HA, mtHMG-CoAS was detected in both the mitochondria and the nucleus. Conversely, when the mutant was co-transfected with mPPARα, its location within the cell remained the same, mitochondrial. Consequently, it appears that mPPARα is required for the translocation of mtHMG-CoAS to the nucleus and its translocation is dependent on the integrity of its LXXLL motif. This defines a novel pathway for PPARα, its use in bringing in mitochondrial proteins to the nucleus.

The amino terminal tagged cHMG-CoAS was found to be non-nuclear. However, the localization of cHMG-CoAS appeared to not be entirely cytoplasmic. It looked like some cHMG-CoAS might actually be in or associated with some kind of organelle within the cytoplasm. The only localization studies done to date on the cytoplasmic enzyme are fractionation studies which have cHMG-CoAS being purified in the cytoplasmic fraction (Clickenbeard *et al.*, 1975a,b). It is also worth noting that the HMG-CoA produced by cHMG-CoAS is utilized by HMG-CoA reductase which is located in the membrane of the endoplasmic reticulum (reviewed in Goldstein and Brown, 1984). The catalytic domain of HMG-CoA is located on the cytoplasmic side of the endoplasmic reticulum. Consequently, one explanation for the localization seen would be that some cHMG-CoAS is loosely associated with the ER in order to be in the proximity of the enzyme which requires its product. Obviously, further work needs to be done to truly identify cHMG-CoAS location within the cell.

4.6 Enzymatic Possibilities

It should also be mentioned that mtHMG-CoAS is an enzyme that becomes acetylated as an intermediate in its catalytic reaction (Rokosz *et al.*, 1994). Consequently, whether its modulating capabilities are at all related to its enzymatic properties have not been properly addressed. It is interesting to note that histone acetylation has been identified as a means of chromatin remodeling and subsequent activation of transcription (Tsukiyama and Wu, 1997). Recently, it has also been determined that acetylation of the actual basal transcriptional machinery may also be another mode of transcriptional regulation (Imhorf *et al.*, 1997). Also, several coactivators have been shown to possess acetylation capabilities such as SRC-1 (Spencer *et al.*, 1997, reviewed in Pazin and Kadonaga, 1997). Consequently, what role mtHMG-CoAS has in acetylating histones, basal transcriptional machinery or any other proteins would prove to be enlightening.

4.7 EMSAs

If the catalytic properties of mtHMG-CoAS were found to be important for its modulating capabilities, this would help to explain the results obtained from the EMSAs. Both mtHMG-CoAS and cHMG-CoAS appeared to behave in a similar but PPRE dependent manner. However, EMSAs occur within an open system and consequently, since both enzymes are capable of performing the same catalytic reaction, perhaps the effect seen in the EMSAs was due to the acetylation properties of the enzyme. Therefore, the ability of mtHMG-CoAS to interact with nuclear receptors in a LXXLL motif dependent manner may only be important for mtHMG-CoAS translocation to the nucleus. Once present in the nucleus, perhaps it is mtHMG-CoAS acetylation capabilities that are

the actual modulating factor. Nevertheless, more work on the importance of the enzymatic properties of mtHMG-CoAS still needs to be done.

4.8 Conclusions

In summary, the results presented here indicate a new and exciting method of gene regulation. The key ketogenic mitochondrial HMG-CoAS enzyme appears to be involved in up regulating its own transcription by acting as a co-regulator of mPPARα. This feedback modulation could provide an important mechanism for amplification of its own transcription during extreme circumstances such as starvation. This same enzyme also appears to down regulate transcription of the AOx gene, an important peroxisomal β-oxidation enzyme. This appears to coincide with evidence that suggests that AOx activity is decreased during starvation. Perhaps, during ketogenesis, the mitochondrial β-oxidation pathway provides the main source of acetyl-CoA.

This work opens the door for looking at other proteins containing a LXXLL motif, not just those proteins classically referred to as coactivators. How mtHMG-CoAS is able to modulate transcription still needs to be examined. Whether it is merely its interacting capabilities or its enzymatic properties that are responsible for its regulatory effects would prove to be both an interesting and exciting discovery.

REFERENCES

Ausubel, F., Brent, R., Kingston, R.E., Moore, D.M., Seidman, J.G., Smith, J.A. and Struhl, K. 1997. Current Protocols in Molecular Biology, J. Wiley & Sons. Inc. Canada.

Boukaftane, Y., Duncan, A., Wang, S., Labuda, D., Robert, M-F., Sarrazin, J., Schappert, K. and Mitchell, G.A. 1994. Human mitochondrial HMG CoA synthase: liver cDNA and partial genomic cloning, chromosome mapping to 1p12-p13, and possible role in vertebrate evolution. Genomics **23:** 552-559.

Braissant, O., Foufelle, F., Scotto, C., Dauça, M. and Wahli, W. 1996. Differential expression of peroxisome proliferator-activated receptors (PPARs): tissue distribution of PPAR-α, -β, and -γ in the adult rat. Endocrin. **137:** 354-366.

Brockman, W.W. and Nathans, D. 1974. The isolation of Simian Virus 40 variants with specifically altered genomes. Proc. Nat. Acad. Sci. **71:** 942-946.

Cavaillès, V., Dauvois, S., L'Horst, F., Lopez, G., Hoare, S., Kushner, P.J. and Parker, M.G. 1995. Nuclear factor RIP140 modulates transcriptional activation by the estrogen receptor. EMBO J. **14:** 3741-3751.

Chen, J.D. and Evans, R.M. 1995. A transcriptional co-repressor that interacts with nuclear hormone receptors. Nature. **377:** 454-457.

Chu, R., Lin, Y., Rao, M.S. and Reddy, J.K. 1996. Cloning and identification of rat deoxyruidine triphosphatase as an inhibitor of peroxisome proliferator-activated receptor α. J. Biol. Chem. **271:** 27670-27676.

Clinkenbeard, K.D., Sugiyama, T., Reed, W.D. and Lane, M.D. 1975a. Cytoplasmic 3-hydroxy-3-methylglutaryl coenzyme A synthase from liver. J. Biol. Chem. **8:** 3124-3135.

Clinkenbeard, K.D., Reed, W.D., Mooney, R.A. and Lane, M.D. 1975b. Intracellular localization of the 3-hydroxy-3-methylglutaryl coenzyme A cycle enzymes in liver. J. Biol. Chem. **8:** 3108-3116.

Danpure, C.J. 1995. How can the products of a single gene be localized to more than one

cellular compartment? Trends Cell Biol. **5:** 230-238.

Devchand, P.R., Keller, H., Peters, J.M., Vazques, M., Gonzalez, F.J. and Wahli, W. 1996. The PPARα-leukotriene B_4 pathway to inflammation control. Nature. **384:** 39-43.

Dowell, P., Ishmael, J.E., Avram, D., Peterson, V.J., Nevrivy, D.J. and Leid, M. 1997a. p300 functions as a coactivator for the peroxisome proliferator-activated receptor α. J. Biol. Chem. **272:** 33435-33443.

Dowell, P., Peterson, V.J., Zabriskie, T.M. and Leid, M. 1997b. Ligand-induced peroxisome proliferator-activated receptor α conformational change. J. Biol. Chem. **272:** 2013-2020.

Dreyer, C., Krey, G., Keller, H., Givel, F., Helftenbein, G. and Wahli, W. 1992. Control of the peroxisomal β-oxidation pathway by a novel family of nuclear hormone receptors. Cell. **68:** 879-887.

Forman, B.M., Tontonoz, P., Chen, J., Brun, R.P., Spiegelman, B.M. and Evans, R.M. 1995. 15-deoxy-$\Delta^{12,14}$-prostaglandin J_2 is a ligand for the adipocyte determination factor PPARγ. Cell. **83:** 803-812.

Fried, M. and Crothers, D.M. 1981. Equilibria and kinetics of lac repressor-operator interactions by polyacrylamide gel electrophoresis. Nuc. Acids. Res. **9:** 6505-6525.

Fujiki, Y., Rachubinski, R.A. and Lazarow, P.B. 1984. Synthesis of a major integral membrane polypeptide of rat liver peroxisomes on free polysomes. Proc. Natl. Acad. Sci. **81:** 7127-7131.

Gil, G., Goldstein, J.L., Slaughter, C.A. and Brown, M.S. 1986. Cytoplasmic 3-hydroxy-3-methylglutaryl coenzyme A synthase from the hamster. J. Biol. Chem. **261:** 3710-3716.

Glass, C.K., Rose, D.W. and Rosenfeld, M.G. 1997. Nuclear receptor coactivators. Curr. Opin. Cell Biol. **9:** 222-232.

Gluzman, Y. 1981. SV40-transformed simian cells support the replication of early SV40 mutrants. Cell. **23:** 175-182.

Goldstein, J.L. and Brown, M.S. 1977. The low-density lipoprotein pathway and its

relation to atherosclerosis. Ann. Rev. Biochem. **46:** 897-930.

Goldstein, J.L. and Brown, M.S. 1984. Progress in understanding the LDL receptor and HMG-CoA reductase, two membrane proteins that regulate the plasma cholesterol. J. Lipid Res. **25:** 1450-1461.

Graham, F.L. and Van Der Eb, A.J. 1973. A new technique for the assay of infectivity of human adenovirus 5 DNA. Virology. **52:** 456-467.

Green, S. 1995. PPAR: a mediator of peroxisome proliferator action. Mut. Res. **333:** 101-109.

Greenspan, M.D., Yudkovitz, J.B., Lo, C.L., Chen, J.S., Alberts, A.W., Hunt, V.M., Chang, M.N., Yang, S.S., Thompson, K.L., Chang, Y-C.P., Chabala, J.C., Monaghan, R.L. and Schwartz, R.L. 1987. Inhibition of hydroxymethylglutaryl-coenzyme A synthase by L-659,699. Proc. Natl. Acad. **84:** 7488-7492.

Greenspan, M.D., Bull, H.G., Yudkovitz, J.B., Hanf, D.P. and Alberts, A.W. 1993. Inhibition of 3-hydroxy-3-methylglutaryl-CoA synthase and cholesterol biosynthesis by β-lactone inhibitors and binding of these inhibitors to the enzyme. Biochem. J. **289:** 889-895.

Guzmán, M. and Geelen, M.J.H. 1993. Regulation of fatty acid oxidation in mammalian liver. Biochim. et Biophys. Acta. **1167:** 227-241.

Handley-Gearhart, P.M., Stephen, A.G., Trausch-Azar, J.S., Ciechanover, A. and Schwartz, A.L. 1994. Human ubiquitin-activating enzyme, *E*1. J. Biol. Chem. **269:** 33171-33178.

Heery, D.M., Kalkhoven, E., Hoare, S. and Parker, M.G. 1997. A signature motif in transcription co-activators mediates binding to nuclear receptors. Nature **387:** 733-736.

Hegardt, F.G. 1995. Regulation of mitochondrial 3-hydroxy-3-methylglutaryl-CoA synthase gene expression in liver and intestine from the rat. Biochem. Soc. Trans. **23:** 486-490.

Hess, R., Stäubli, W. and Riess, W. 1965. Nature of the hepatomegalic effect produced by ethyl-chlorophenoxy-isobutyrate in the rat. Nature **208:** 856-861.

Hong, H., Kohli, K., Trivedi, A., Johnson, D.L. and Stallcup, M.R. 1996. GRIP1, a novel mouse protein that serves as a transcriptional coactivator in yeast for the hormone binding domains of steroid receptors. Proc. Natl. Acad. Sci. **93:** 4948-4952.

Hörlein, A.J., Näär, A.M., Heinzel, T., Torchia, J., Gloss, B., Kurokawa, R., Ryan, A., Kamei, Y., Söderstrom, M., Glass, C.K. and Rosenfeld, M.G. 1995. Ligand-independent repression by the thyroid hormone receptor mediated by a nuclear receptor co-repressor. Nature **377:** 397-404.

Imhorf, A., Yang, X-J., Ogryzko, V.V., Nakatani, Y., Wolffe, A.P. and Ge, H. 1997. Acetylation of general transcription factors by histone acetyltransferases. Curr. Biol. **7:** 689-692.

Kamei, Y., Xu, L., Heinzel, T., Torchia, J., Kurokawa, R., Gloss, B., Lin, S-C., Heyman, R.A., Rose, D.W., Glass, C.K. and Rosenfeld, M.G. 1996. A CBP integrator complex mediates transcriptional activation and AP-1 inhibition by nuclear receptors. Cell. **85:** 403-414.

Kliewer, S.A., Lenhard, J.M., Wilson, T.M., Patel, I., Morris, D.C. and Lehmann, J.M. 1995. A prostaglandin J_2 metabolite binds peroxisome proliferator-activated receptor γ and promotes adipocyte differentiation. Cell. **83:** 813-819.

Korzus, E., Torchia, J., Rose, D.W., Xu, L., Kurokawa, R., McInerney, E.M., Mullen, T-M., Glass, C.K. and Rosenfeld, M.G. 1998. Transcription factor-specific requirements for coactivators and their acetyltransferase functions. Science. **279:** 703-707.

Krey, G., Braissant, O., L'Horst, F., Kalkhoven, E., Perroud, M., Parker, M.G. and Wahli, W. 1997. Fatty acids, eicosanoids, and hypolipidemic agents identified as ligands of peroxisome proliferator-activated receptors by coactivator-dependent receptor ligand assay. Mol. Endocrin. **11:** 779-791.

Lehmann, J.M., Moore, L.B., Smith-Oliver, T.A., Wilkison, W.O., Wilson, T.M. and Kliewer, S.A. 1995. An antidabetic thiazolidinedione is a high affinity ligand for peroxisome proliferator-activated receptor γ (PPARγ). J. Biol. Chem. **270:** 12953-12956.

Lemberger, T., Desvergne, B. and Wahli, W. 1996. Peroxisome proliferator-activated receptors: a nuclear receptor signaling pathway in lipid physiology. Annu. Rev. Cell. Dev. Biol. **12:** 335-353.

Lock, E.A., Mitchell, A.M. and Elcombe, C.R. 1989. Biochemical mechanisms of induction of hepatic peroxisome proliferation. Annu. Rev. Pharmacol. Toxicol. **29:** 145-163.

Mangelsdorf., D.J. and Evans, R.M. 1995. The RXR heterodimers and orphan receptors. Cell. **83:** 841-850.

Marcus, S.L., Miyata, K.S., Zhang, B., Subramani, S., Rachubinski, R.A. and Capone, J.P. 1993. Diverse peroxisome proliferator-activated receptors bind to the peroxisome proliferator-responsive elements of the rat hydratase/dehydrogenase and fatty acyl-CoA oxidase genes but differentially induce expression. Proc. Natl. Acad. Sci. **90:** 5723-5727.

Mascaró, C., Buesa, C., Ortiz, J.A., Haro, D. and Hegardt, F.G. 1994. Molecular cloning and tissue expression of human mitochondrial 3-hydroxy-3-methylglutaryl-CoA synthase. Arch. Biochem. Biophys. **317:** 385-390.

Mayer, R.J., Louis-Flamberg, P., Elliott, J.D., Fisher, M. and Leber, J. 1990. Inhibition of 3-hydroxy-3-methylglutaryl coenzyme A synthase by antibiotic 1233A and other β-lactones. Biochem. and Biophys. Res. Comm. **169:** 610-616.

McGarry, J.D. and Foster, D.W. 1980. Regulation of hepatic fatty acid oxidation and ketone body production. Ann. Rev. Biochem. **49:** 395-420.

Miyata, K.S., McCaw, S.E., Marcus, S.L., Rachubinski, R.A. and Capone, J.P. 1994. The peroxisome proliferator-activated receptor interacts with the retinoid X receptor *in vivo*. Gene. **148:** 327-330.

Miyata, K.S., McCaw, S.E., Patel, H.V., Rachubinski, R.A. and Capone, J.P. 1996. The orphan nuclear hormone receptor LXRα interacts with the peroxisome proliferator-activated receptor and inhibits peroxisome proliferator signaling. J. Biol. Chem. **271:** 9189-9192.

Miyata, K.S., McCaw, S.E., Meertens, L.M., Patel, H.V., Rachubinski, R.A. and Capone, J.P. 1998. Receptor-interacting protein 140 interacts with, and inhibits transactivation by, peroxisome proliferator-activated receptor α and liver-X-receptor α. Submitted.

Nagashima, H., Kumagai, H., Tomoda, H. and Ōmura, S. 1993. Inhibition of hepatic

cholesterol biosynthesis by a 3-hydroxy-3-methylglutaryl coenzyme A synthase inhibitor, 1233A, in mice. Life Sci. **52:** 1595-1600.

Oñate, S.A., Tsai, S.Y., Tsai, M-J. and O'Malley, B.W. 1995. Sequence and Characterization of a coactivator for the steroid hormone receptor superfamily. Science. **270:** 1354-1357.

Paget, G.E. 1963. Experimental studies of the toxicity of atromid with particular reference to fine structural changes in the livers of rodents. J. Ather. Res. **3:** 729-736.

Pazin, M.J. and Kadonaga, J.T. 1997. What's up and down with histone deacetylation and transcription? Cell. **89**: 325-328.

Puigserver, P., Wu, Z., Park, C.W., Graves, R., Wright, M. and Spiegelman, B.M. 1998. A cold-inducible coactivator of nuclear receptors linked to adaptive thermogenesis. Cell. **92:** 829-839.

Reed, W.D., Clinkenbeard, K.D. and Lane, M.D. 1975. Molecular and catalytic properties of mitochondrial (ketogenic) 3-hydroxy-3-methylglutaryl coenzyme A synthase of liver. J. Biol. Chem. **8:** 3117-3123.

Rodríguez, J.G., Gil-Gomez, G., Hegardt, F.G. and Haro, D. 1994. Peroxisome proliferator-activated receptor mediates induction of the mitochondrial 3-hydroxy-3-methylglutaryl-CoA synthase gene by fatty acids. J. Biol. Chem. **269:** 18767-18772.

Rodríguez, J.C., Rotiz, J.A., Hegardt, F.G. and Haro, D. 1997. Chicken ovalbumin upstream-promoter transcription factor (COUP-TF) could act as a transcriptional activator or repressor of the mitochondrial 3-hydroxy-3-methylglutaryl-CoA synthase gene. Biochem. J. **326:** 587-592.

Rodríguez, J.C., Ortiz, J.A., Hegardt, F.G. and Haro, D. 1998. The hepatocyte nuclear factor 4 (HNF-4) represses the mitochondrial HMG-CoA synthase gene. Biochem. and Biophys. Res. Comm. **242:** 692-696

Rokosz, L.L., Boulton, D.A., Butkiewicz, E.A., Sanyal, G., Cueto, M.A., Lachance, P.A. and Hermes, J.D. 1994. Human cytoplasmic 3-hydroxy-3-methylglutaryl coenzyme A synthase:expression, purification, and characterization of recombinant

wild-type and Cys^{129} mutant enzymes. Arch. Biochem. Biophys. **312:** 1-13.

Royo, T., Pedragose, M.J., Ayté, J., Gil-Gómez, G., Vilaró, S. and Hegardt, F.G. 1995. Immunolocalization of mitochondrial 3-hydroxy-3-methylglutaryl CoA synthase in rat liver. J. Cell. Phys. **162:** 103-109.

Sambrook, J., Fritsch, E.F. and Maniatis, T. 1989. Molecular Cloning a Laboratory Manual. Cold Spring Harbor Laboratory Press. Edited by C. Nolan. U.S.A.

Schoonjans, K., Staels, B. and Auwerx, J. 1996a. The peroxisome proliferator activated receptors (PPARs) and their effects on lipid metabolism and adipocyte differentiation. Biochem. et Biophys. Acta **1302:** 93-109.

Schoonjans, K., Staels, B. and Auwerx, J. 1996b. Role of the peroxisome proiferator-activated receptor (PPAR) in mediating the effects of fibrates and fatty acids on gene expression. J. Lipid Res. **37:** 907-925.

Shibata, H., Spencer, T.E., Oñate, Jenster, G., Tsai, S.Y., Tsai, M-J. and O'Malley, B.W. 1997. Role of co-activators and co-repressors in the mechanism of steroid/thyroid receptor action. Endocrine Soc. **52:** 141-165.

Slauter, R.W. and Yamazaki, R.K. 1984. Glucagon and fasting do not activate peroxisomal fatty acid β-oxidation in rat liver. Arch. Biochem. Biophys. **233:** 197-202.

Soltys, B.J. and Gupta, R.S. 1996. Immunoelectron microscopic localization of the 60-kDa heat shock chaperonin protein (Hsp60) in mammalian cells. Exper. Cell Res. **222:** 16-27.

Spencer, T.E., Jenster, G., Burcin, M.M., Allis, C.D., Zhou, J., Mizzen, C.A., McKenna, N.J., Onate, S.A., Tsai, S.Y., Tsai, M-J. and O'Malley, B.W. 1997. Steroid receptor coactivator-1 is a histone acetyltransferase. Nature. **389:** 194-198.

Tomoda, H., Kumagai, H., Takahashi, Y., Tanaka, Y., Iwai, Y. and Ōmura, S. 1987. F-244 (1233A), a specific inhibitor of 3-hydroxy-3-methylglutaryl coenzyme A synthase: taxonomy of producing strain, fermentation, isolation and biological properties. J. Ant. **41:** 247-249.

Tontonoz, P., Hu, E., Graves, R.A., Budavari, A.I. and Spiegelman, B.M. 1994. mPPARγ2: tissue-specific regulator of an adipocyte enhancer. Genes & Devel. **8:**

81224-81234.

Tontonoz, P., Hu, E., Graves, R.A. and Spiegelman, B.M. 1994. Stimulation of adipogenesis in fibroblasts by PPARγ2, a lipid-activated transcription factor. Cell. **79:** 1147-1156.

Torchia, J., Rose, D.W., Inostroza, J., Kamei, Y., Westin, S., Glass, C.K. and Rosenfeld, M.G. 1997. The transcriptional co-activator p/CIP binds CBP and mediates nuclear-receptor function. Nature **387:** 677-684.

Tsukiyama, T., and Wu, C. 1997. Chromatin remodeling and transcription. Curr. Opin. Gen. Devel. **7:** 182-191.

Tugwood, J.D., Issemann, I., Anderson, R.G., Bundell, K.R., McPheat, W.L. and Green, 1992. The mouse peroxisome proliferator activated receptor recognizes a response element in the 5′ flanking sequence of the rat acyl CoA oxidase gene. EMBO J. **11:** 433-439.

Varanasi, U., Chu, R., Huang, Q., Castellon, R., Yeldandi, A.V. and Reddy, J.K. 1996. Identification of a peroxisome proliferator-responsive element upstream of the human peroxisomal fatty acyl coenzyme A oxidase gene. J. Biol. Chem. **271:** 2147-2155.

Voegel, J.J., Heine, M.J.S., Zechel, C., Chambon, P. and Gronemeyer, H. 1996. TIF2, a 160 kDa transcriptional mediator for the ligand-dependent activation function AF-2 of nuclear receptors. EMBO. **15:** 3667-3675.

Wurtz, J-M., Bourguet, W., Renaud, J-P., Vivat, V., Chambon, P., Moras, D. and Gronemeyer, H. 1996. A canonical structure for the ligand-binding domain of nuclear receptors. Nat. Struct. Biol. **3:** 87-94.

Yang, X-J., Ogryzko, V.V., Nishikawa, J-i., Howard, B.H. and Nakatani, Y. 1996. A p300/CBP-associated factor that competes with the adenoviral oncoprotein E1A. Nature. **382:** 319-324.

Zhang, B., Marcus, S.L., Sajjadi, F.G., Alvares, K., Reddy, J.K., Subramani, S., Rachubinski, R.A. and Capone, J.P. 1992. Identification of a peroxisome proliferator-responsive element upstream of the gene encoding rat peroxisomal enoyl-CoA hydratase/3-hydroxyacyl-CoA dehydrogenase. Proc. Natl. Acad. Sci. **89:** 7541-7545.

Zhu, Y., Alvares, K., Huang, Q., Rao, M.S. and Reddy, J.K. 1993. Cloning of a new member of the peroxisome proliferator-activated receptor gene family from mouse liver. J. of Biol. Chem. **268:** 26817-26820.

Zhu, Y., Qi, C., Korenberg, J.R., Chen, Z-N., Noya, D., Rao, M.S. and Reddy, J.K. 1995. Structural organization of mouse peroxisome proliferator-activated receptor γ (mPPARγ) gene: alternative promoter use and different splicing yield two mPPARγ isoforms. Proc. Natl. Acad. Sci. **92:** 7921-7925.

Zhu, Y., Qi, C., Calandra, C., Rao, M.S. and Reddy, J.K. 1996. Cloning and identification of mouse receptor coactivator-1 (mSRC-1), as a coactivator of peroxisome proliferator-activated receptor γ. Gene Expr. **6:** 185-195.

Zhu, Y., Qi, C., Jain, S., Rao, M.S. and Reddy, J.K. 1997. Isolation and characterization of PBP, a protein that interacts with peroxisome proliferator-activated receptor. J. Biol. Chem. **272:** 25500-25506.